Progress in Aerospace Sciences ∎ (∎∎∎∎) ∎∎∎–∎∎∎

Contents lists available at ScienceDirect

Progress in Aerospace Sciences

journal homepage: www.elsevier.com/locate/paerosci

Free underexpanded jets in a quiescent medium: A review

Erwin Franquet [a,b,*], Vincent Perrier [b,c], Stéphane Gibout [a], Pascal Bruel [d,b]

[a] LaTEP-ENSGTI, Univ. Pau & Pays Adour, Bâtiment d'Alembert, rue Jules Ferry, 64 075 Pau Cedex, France
[b] Inria Cagire team, 200 rue Vieille Tour, 33 405 Talence Cedex, France
[c] LMAP, UMR CNRS 5142, Univ. Pau & Pays Adour, France
[d] CNRS, Univ. Pau & Pays Adour, LMAP, UMR CNRS 5142, France

ARTICLE INFO

Article history:
Received 29 April 2015
Received in revised form
24 June 2015
Accepted 25 June 2015

Keywords:
Underexpanded jet
Singular reflection
Potential core
Mach disk
Farfield zone
Asymptotic zone
Similarity laws
Equivalent diameter
Notional nozzle

ABSTRACT

When dealing with high-pressure releases, be it needed by some operating conditions or due to an emergency protocol or even to the occurrence of an accident, one has to consider the relevant risks associated to this leakage. Indeed, in addition to the mechanical and blast effects, the dispersion of the released fluid is of primary importance if it is hazardous, as an example for toxic gases or flammable ones (where explosions or fires may be expected).

In fact, despite the numerous studies dealing with underexpanded jets, many aspects of their structure are not clearly described, particularly when one seeks for quantitative predictions. By performing an exhaustive overview of the main experimental papers dealing with underexpanded jets, the present paper aims at clarifying the characteristics which are well known, from those where there is clearly a lack of confidence. Indeed, and curiously enough, such a work has never been done and no review is available on such a topic.

Two particular regions have drawn most of the attention so far: the nearfield zone, where the shocks/rarefaction pattern that governs the structure of the jet is encountered, and the farfield zone, where the flow is fully developed and often approximated by an equivalent flow.

Finally, some clues are given on the numerical methods that may be used if one wants to study such jets numerically, together with an emphasis on the specific thermodynamical difficulties associated to this kind of extreme conditions.

Contents

* Corresponding author at: LaTEP-ENSGTI, Univ. Pau & Pays Adour, Bâtiment d'Alembert, rue Jules Ferry, 64 075 Pau Cedex, France. Fax: +33 559407725.
E-mail address: erwin.franquet@univ-pau.fr (E. Franquet).

http://dx.doi.org/10.1016/j.paerosci.2015.06.006
0376-0421/

1. Introduction

Historically, the underexpanded jets have long been studied, particularly by some of the most famous scientists [1–8]. They are involved in practical engineering and challenging situations, such as exhaust and plumes of aircrafts and rockets (where the thermal signature, jet noise and screech or flow behavior were studied), and mixing issues in supersonic combustors or parallel injection, and accidental leakage of pressurized fluid, etc. In each of these situations, the main features concerning the risk prediction and control are linked to the overall structure of the jet, that is to say the pressure (or temperature, or velocity) levels attained in its surrounding, and to the knowledge of the concentration evolution, which permits a comparison with some physical criterion (such as the permissible exposure limits or the inflammability limits). Generally, one distinguishes between the free jets and the impacting ones, and the exhausted fluid may be released either in a quiet medium or in a moving one (i.e. a coflow jet or a jet in crossflow). Besides, the jet may be either axi-symmetric or present an asymmetry. The present review will concentrate on the former configuration.

Nowadays, thanks to all the associated papers, the overall structure of underexpanded jets is very well known. Yet, in spite of the large amount of studies that has been published, many characteristic features or quantitative aspects are still ill-known or even ignored by those numerous publications, e.g. the curvature of the Mach disk, the characteristic lengths of the jet in the supersonic case or with various jet/ambient fluids, the position where entrainment arises, the turbulent transition in the mixing layer, the interactions between hydrodynamic instabilities and the shock waves pattern, the fine and complete structure of turbulent vortices, the method to correctly approximate the flow in the farfield region, etc. Moreover, there sometimes exists a large scattering between the different measurements, which are even sometimes occasionally in contradiction.

In order to have a fair view of the reliable results among all the available studies, the goal of this paper is thus to propose an exhaustive analysis of the open literature on axi-symmetric free underexpanded jets by comparing the qualitative and also quantitative predictions proposed therein. Thereby, the aim is to know exactly in which characteristics and associated correlations we may have confidence in. Let us mention here that we are mainly considering experimental studies.

The paper is organized as follows: in Section 2, a brief summary is given on the physical appearance of axi-symmetric under-expanded jets, and their global structure is presented in Section 3. Then, a deeper description of the potential zone (nearfield region) and of the fully developed one (farfield zone) is given in Sections 4 and 5. Finally, an overview of the numerical models and methods that may be used to further improve our knowledge of the underexpanded jets is proposed in Section 6. The possible issues raised by the thermodynamical behavior of the fluid are addressed in Section 7.

2. Forewords

An underexpanded jet may occur whenever a fluid is released from a device at a pressure greater than the ambient pressure. It is known from a long time that such a behavior arises with convergent and convergent–divergent nozzles (holes being a particular case of these ones), as recalled in [9–11].

For a convergent nozzle, two main situations may be encountered, depending on the initial pressure of the fluid or, more precisely, on the ratio between the total pressure of the fluid and that of the ambient atmosphere. Thus, two different regimes with different evolutions of the pressure inside the device are encountered, as depicted in Fig. 1. The associated evolutions of the

Please cite this article as: E. Franquet, et al., Free underexpanded jets in a quiescent medium: A review, Progress in Aerospace Sciences (2015), http://dx.doi.org/10.1016/j.paerosci.2015.06.006

Notation

Latin Letters

a	virtual origin (m)
A	area (m^2)
c	sound velocity ($m\ s^{-1}$)
c_p	specific heat capacity ($J\ K^{-1}\ kg^{-1}$)
C_D	discharge coefficient (–)
D	diameter (m)
h	specific enthalpy ($J\ kg^{-1}$)
Kn	Knudsen number (–)
L	length (m)
M	Mach number (–)
P	pressure (Pa)
$\hat{R}$	universal ideal gas constant ($J\ K^{-1}\ mol^{-1}$)
R	relative ideal gas constant ($J\ K^{-1}\ kg^{-1}$)
r	radial position (m)
Re	Reynolds number (–)
T	temperature (K)
V	velocity ($m\ s^{-1}$)
v	specific volume ($m^3\ kg^{-1}$)
x	longitudinal position (m)
Y	mass fraction (–)

Greek Letters

α	volume fraction (–)
β	nozzle angle (°)
γ	polytropic coefficient (–)
ζ	decay constant (–)
κ	decay constant (–)
λ	wavelength (m)
η	pressure ratio (–)
ρ	density ($kg\ m^{-3}$)
ν	Prandtl–Meyer angle (°)
θ	divergence angle of the jet (°)

Superscripts and subscripts

0	stagnation (or total) state
∞	ambient conditions
*	critical state (i.e. sonic flow)
¢	cell
c	critical point (thermodynamical definition)
e	exit plane
eq	equivalent
id	ideally expanded
t	throat

Abbreviations

CV	convergent
CV–DV	convergent–divergent
KH	Kelvin–Helmholtz
MD	Mach disk
NZ	nearfield zone
RR	regular reflection
SR	singular reflection
TZ	transition zone
TP	triple point
TG	Taylor–Goertler
FZ	farfield zone

mass flow and exit pressure are also shown in Fig. 2(a) and (b). The first regime corresponds to the subsonic case, where the exit pressure is equal to the ambient pressure and the mass flow increases with the initial pressure (cases a and b). In the second one, the critical state where the flow becomes sonic (case c) is attained, the nozzle is now choked: the exit pressure is equal to the critical pressure and the mass flow is maximal. Except for the marginal effects due to the presence of the boundary layer, the flow now mainly depends on the total conditions. Above this point, all the variables have the same behavior inside the nozzle (case d) yet the exit pressure is now greater than the ambient pressure: pressure equilibrium will occur outside the device and therefore it gives rise to an underexpanded jet.

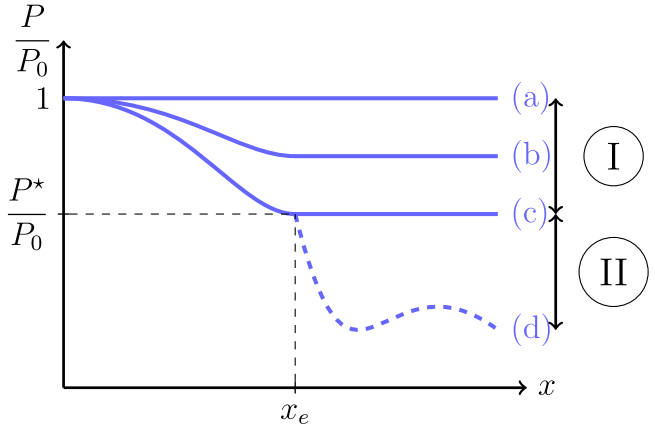

Fig. 1. Longitudinal pressure evolution in a convergent nozzle for various pressure ratios.

For a convergent–divergent nozzle, the longitudinal pressure evolution, the mass flow and the exit pressure are also presented in Figs. 3 and 4. As in the previous case, the flow is first subsonic (case b) where the exit pressure equals the ambient pressure and the mass flow is governed by the ratio between the total pressure and the ambient pressure. Then, the choked state (cases c–g) is attained: the flow is sonic at the throat and the mass flow only depends on the total conditions (ignoring once more the small effects due to viscous phenomena). From now, except for the design operating conditions (case e), the exit pressure will be different from the ambient pressure: if it is lower (case f) it corresponds to an overexpanded jet, otherwise (case g) it is an underexpanded jet.

To quantitatively assess the appearance of an underexpanded jet, the following pressure ratios are defined

$$\eta_0 = \frac{P_0}{P_\infty} \tag{1}$$

$$\eta_e = \frac{P_e}{P_\infty} \tag{2}$$

From the above discussion, underexpansion appears only if

$$\eta_0 \geq \frac{P_0}{P^\star} \tag{3}$$

When dealing with CV–DV nozzles, a supplementary condition is required:

$$\eta_e > 1 \tag{4}$$

Please cite this article as: E. Franquet, et al., Free underexpanded jets in a quiescent medium: A review, Progress in Aerospace Sciences (2015), http://dx.doi.org/10.1016/j.paerosci.2015.06.006

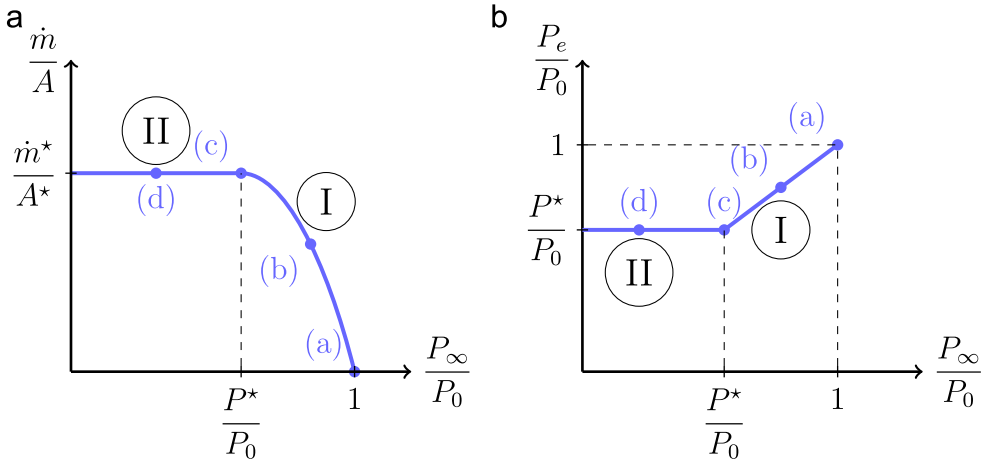

Fig. 2. Evolution of the variables in a convergent nozzle for various pressure ratios: (a) mass flow and (b) exit pressure.

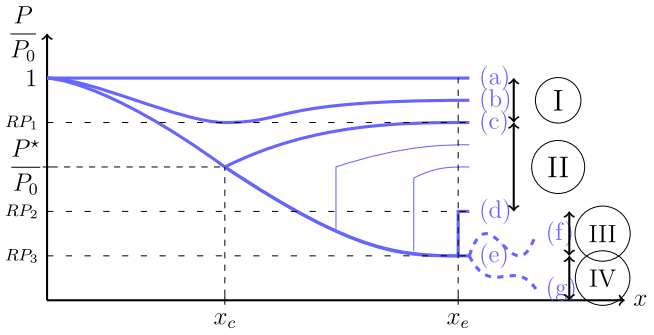

Fig. 3. Longitudinal pressure evolution in a convergent–divergent nozzle for various pressure ratios.

Generally, the differences between various gases are quite small [12–14] and the previous method gives reliable results. Nonetheless, the perfect gas equation of state is not able to deal with all the situations or fluids and may not perfectly describe the thermodynamical behavior of the flow in such a case. To improve the results, and better describe the real behavior of the fluid, one may incorporate a discharge coefficient C_D (detailed in Appendix C) to better estimate the mass-flow rate or study the influence of the equation of state on the properties of the fluid at the throat and/or at the exit of the nozzle (see Section 7 for further information).

3. Structure of the jet

3.1. General features

As mentioned previously, an underexpanded jet occurs when the pressure at the end of a device, may it a nozzle or a hole, is greater than the ambient pressure. The transient behavior of the fluid has not focused attention of many studies, be it theoretical [15] or experimental [16–19] or numerical [17,18,20–26] ones. On the contrary, the steady state of the flow has been largely studied in the past [27–53] , since it corresponded to the most often encountered situations. To briefly summarize its main characteristics, the compressible and viscous effects compete together to impose the overall structure of the jet. Generally, it is usual to distinguish three zones inside the jet:

1. the nearfield zone;
2. the transition zone;
3. the farfield zone.

The nearfield zone is divided into two parts: the core part and the mixing layer. In the first one, the flow is isolated from the ambient fluid and its behavior is mainly dominated by compressible effects (which explains why this zone is sometimes called the gas-dynamic region). The fluid undergoes an isentropic expansion, up to recompression through shock waves (described farther downstream). In the other part, turbulence effects induce an exchange

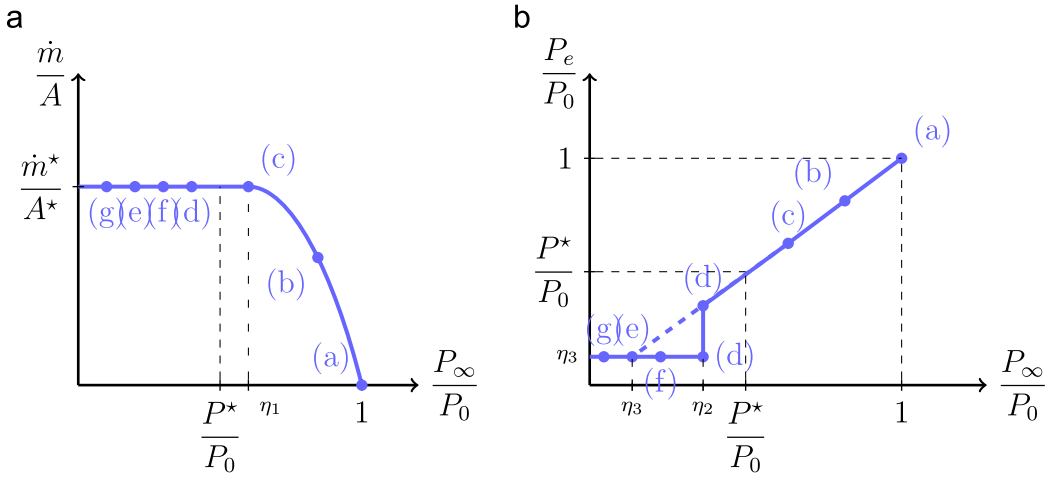

Fig. 4. Evolution of the variables in a convergent–divergent nozzle for various pressure ratios: (a) mass flow and (b) exit pressure.

Please cite this article as: E. Franquet, et al., Free underexpanded jets in a quiescent medium: A review, Progress in Aerospace Sciences (2015), http://dx.doi.org/10.1016/j.paerosci.2015.06.006

between the ejected fluid and the surrounding one, characterized by large turbulent structures (vortex) which grow regularly downstream of the flow. In this shearing zone, a supersonic part, between the frontier of the jet and the constant pressure line, and a subsonic one, between this line and the potential core, may be distinguished. At the end of the nearfield zone, the sonic line attains the axis and therefore the mixing layer has completely replaced the inner part. Then, it corresponds to the beginning of the transition zone where the variations of the variables are small, be it longitudinally or radially. This permits a better mixing of the two fluids, the ejected one and the ambient one, leading to a homogenization of the pressure field since the entrainment now takes place everywhere.

Eventually, in the farfield zone, the jet is perfectly expanded, the flow is developed and its characteristics (mean pressure, temperature and velocity) are self-similar. The longitudinal velocity and the temperature on the axis are inversely proportional to the distance from the exit plane, and their radial evolution may be described by a gaussian profile centered on the axis. Let us mention here that depending on the various communities, and especially those involved in hydrogen (or combustible gas) safety or those from the turbulence field, one sometimes split this zone into two others: a momentum-dominated one followed by a buoyancy-controlled regime which are characterized by different Froude number.

3.2. Nearfield zone

In this region, the flow is mainly governed by the compressible effects and is rather steady. Practically, the relevant parameter is the pressure ratio. Moreover, the exit Mach number and the divergence angle of the jet in the exit plane may have some influence. Thus, four different situations are possible:

1. under-expansion of the fluid is low, a normal shock is present in the exit plane. Typically, for air, it corresponds to $1 \leq \eta_e \leq 1.1$ [34] or to $1 \leq \eta_0 \leq 1.9$ [38].
2. the jet has a “diamond” or “X” structure, depicted in Fig. 5, which corresponds to a moderately underexpanded jet detailed hereafter.
3. the jet has a “barrel” or “bottle” structure, shown in Fig. 6, meaning a Mach disk appears (due to a singular reflection). It corresponds now to a highly underexpanded jet also described below.
4. the structure is dominated by a unique barrel, as depicted in Fig. 7, and the jet is said to be very highly (or extremely) underexpanded.

Moderately underexpanded jet (*see* Fig. 5): In the exit plane (marker 0), a Prandtl–Meyer expansion fan (marker 2) expands the fluid downstream of the lips of the device up to the jet boundary corresponding to the external surface of the mixing layer (marker JB). When these acoustic waves attain the constant pressure streamline (marker 3), where the pressure equals the ambient pressure, they are reflected into compression waves. Then, these ones converge towards the inner jet and coalesce to form an oblique shock (marker 4), usually called the intercepting shock. On the axis, this incident shock itself reflects in a new oblique shock, the reflected shock (marker 5), facing the outer jet. Eventually, when this shock wave encounters the constant pressure streamline it gives birth to a new expansion fan (marker 6) which permits us to replicate the cell structure further downstream. In the case of air, this situation is achieved for an exit pressure ratio $1.1 \lesssim \eta_e \lesssim 3$ [34,38,54] or for a total pressure ratio $2 \lesssim \eta_0 \lesssim 4$ [38,13,55].

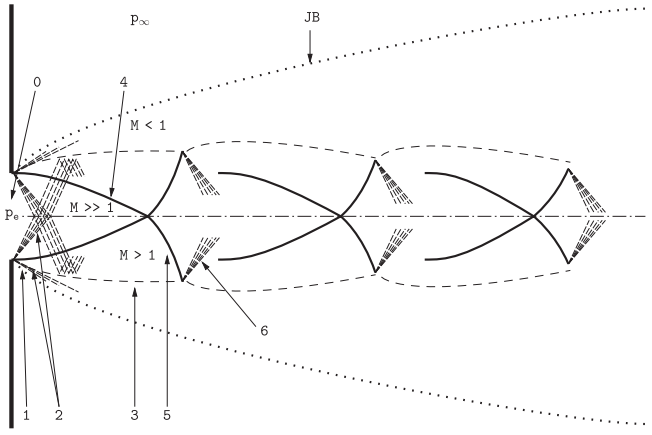

Fig. 5. Structure of a moderately underexpanded jet.

Highly underexpanded jet (*see* Fig. 6): When the pressure ratio increases, the regular reflection of the intercepting shock can no longer happen on the axis. Consequently, above a critical angle, this reflection becomes singular and leads to the apparition of a normal shock, called the Mach disk (marker 5). There, the point where the intercepting shock, the Mach disk and the reflected shock intersect themselves (marker 6) is called the triple point. A slipstream (marker 7) then emanates from this point: this is an embedded shear layer separating the flow behind the Mach disk (which is subsonic) from the flow downstream of the reflected shock (which is supersonic). Typically, this corresponds to an exit pressure ratio $2 \lesssim \eta_e \lesssim 4$ [30,34,38,56–61,43,54] or to a total pressure ratio $4 - 5 \lesssim \eta_0 \lesssim 7$ [62–65,35,38,59,13].

Very highly (*extremely*) *underexpanded jet* (*see* Fig. 7): With a further increase of the pressure ratio, the number of shock cells diminishes up to a point where the potential core is dominated by the first cell, this one being unique and no other structures being formed. In such a case, the Mach disk can no longer be considered as a normal shock and its curvature has to be taken into account. The total diameter of the jet will diminish due to momentum exchange, caused by the entrainment of the ambient fluid, leading to a very long plume. Typically, this corresponds to an exit pressure ratio $3 - 4 \lesssim \eta_e$ [57,43] or to a total pressure ratio $\eta_0 \geq 7$ [35].

3.3. Farfield zone

In this region, the jet has achieved a self-similarity, yet compressible effects may still be present since the Mach number may be greater than 0.3 (or even supersonic). From a qualitative point of view, the normalized radial profiles of the mean variables obey the same law (usually given by a Gaussian profile).

Nevertheless, it appears that in this region one may describe the flow as a classical jet, i.e. as an ideally expanded jet, by scaling some of the basic flow parameters. Indeed, it does not matter anymore here how exactly the fluid comes to this state, which means that it is not mandatory to have a perfect description of the nearfield zone and of the associated structure (shock wave pattern, number of Mach disks, etc.). The point is that one has to deal with a supersonic jet, behaving as classical jets but apparently coming from a larger source than the real one. This is the only testimony of its original underexpanded feature. In Section 5, this zone will be further described along with the various description approaches of the jet behavior.

4. Potential core of a highly underexpanded jet

The main goal of this section is to detail the characteristics of highly and extremely underexpanded jets, where a singular reflexion occurs. In particular, to have a fair view of the different features,

Please cite this article as: E. Franquet, et al., Free underexpanded jets in a quiescent medium: A review, Progress in Aerospace Sciences (2015), http://dx.doi.org/10.1016/j.paerosci.2015.06.006

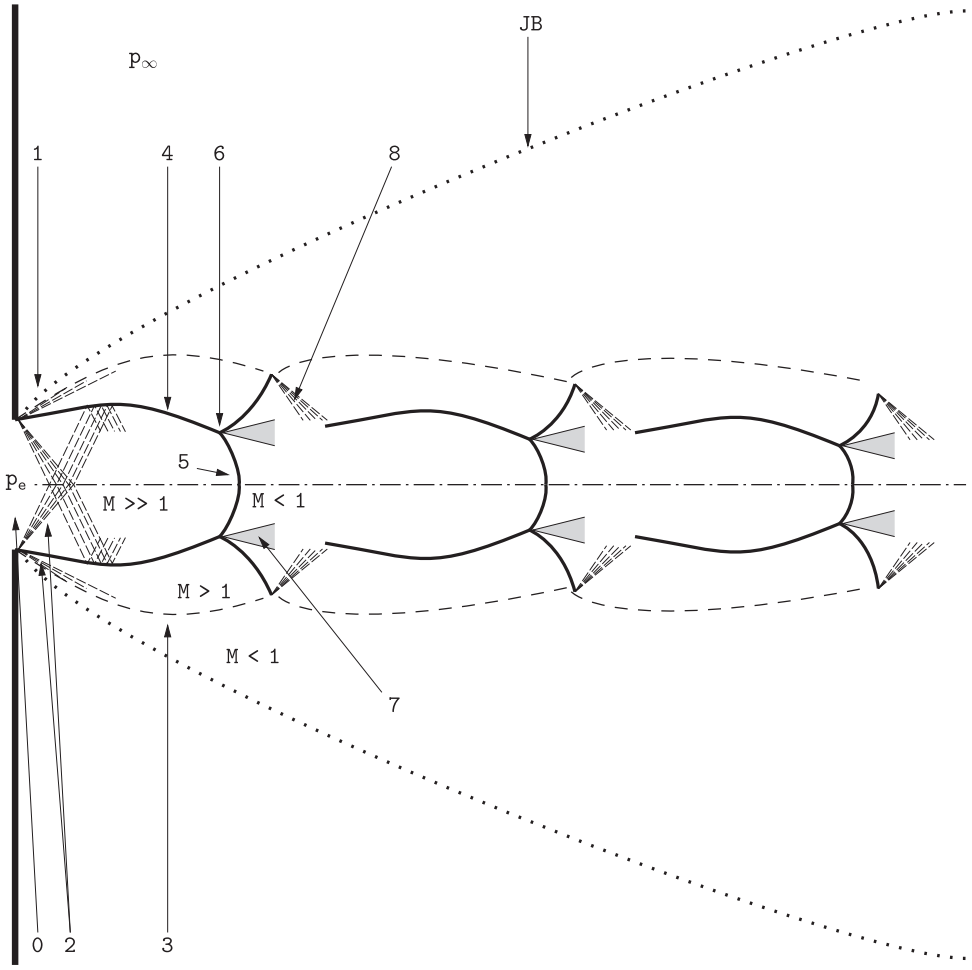

Fig. 6. Structure of a highly underexpanded jet.

quantitative and theoretical results (whenever available) are presented and discussed. A summary of all the available results is presented in Table 2.

4.1. The Mach disk

This is certainly the most studied feature in the literature, be it experimentally [12,30,35,40,43,49,51,56–59,62,64,66–94], theoretically [13,29,67,76,78,95–109] or numerically [14,20,22,34,41,59,63,75,81,82,84,91,110–122].Yet, if one tries to understand the reason for the appearance of a Mach disk, there is still some doubt about the underlying physical mechanisms. More precisely, in the passage from a regular reflection to a singular reflection, accompanied by the appearance of the Mack disk, it is well known that the detachment of the shock waves occurs because this is the only way for the flow to adjust to a subsonic regime [10, Chap. 16] or [11, Chap. 7] but the moment when this phenomenon occurs is quantitatively poorly known, especially the dependency (and interactions) on the pressure

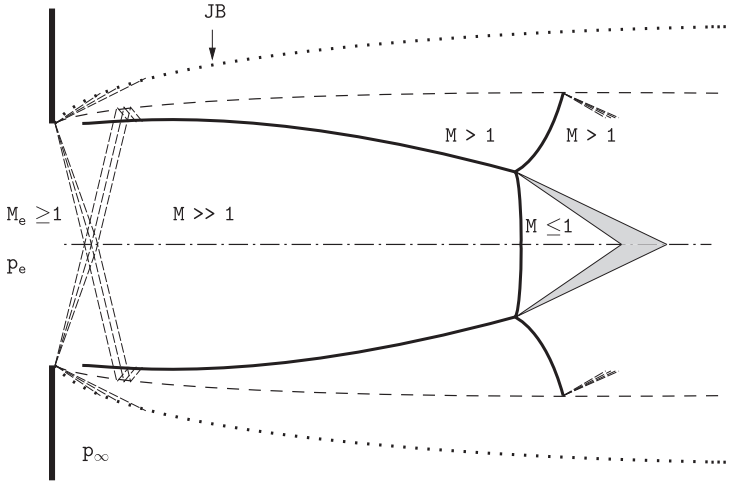

Fig. 7. Structure of a very highly underexpanded jet.

Please cite this article as: E. Franquet, et al., Free underexpanded jets in a quiescent medium: A review, Progress in Aerospace Sciences (2015), http://dx.doi.org/10.1016/j.paerosci.2015.06.006

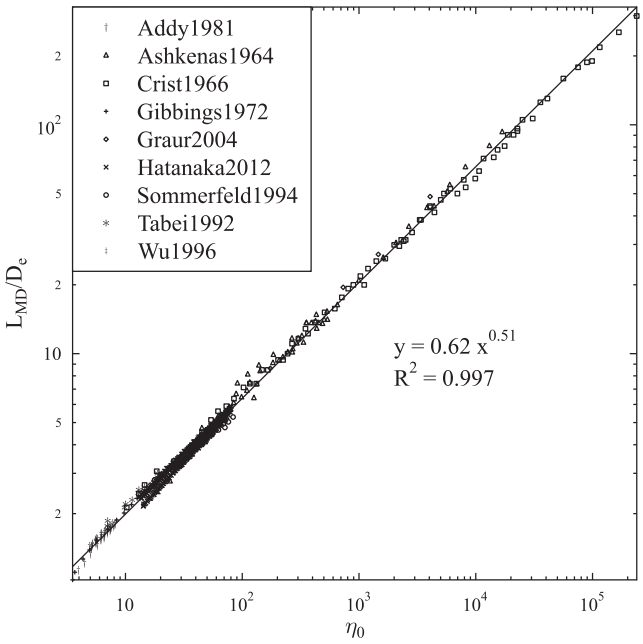

Fig. 8. Position of the Mach disk in function of the total pressure ratio.

range and exit Mach number, on the fluid properties – i.e. the polytropic coefficient – on the geometry of the nozzle and exit nozzle angle [96,29,62,30,98–100,12,64,123,43,124,84,13,107,90,54]. Nonetheless, among the theoretical studies, the Mach disk location has been supposed to appear at a position such that

- the conservation equations are satisfied for the section perpendicular to the axis [95].
  This hypothesis has the advantage to rely on physical backgrounds, yet some discrepancies appear when compared with the experiments. They are supposed to come from viscous effects that are ignored.
- The associated slip line will permit a correct re-acceleration of the flow downstream [96,106,107].
  From [107,108], this leads to the best results when compared with the experiments.
- It corresponds to a normal shock bringing the static pressure to the ambient pressure [29].
  As mentioned in [100], if true, it will be the case only for the last Mach disk.
- The Mach disk is a normal shock at the triple point [98].
- The static pressure behind the intercepting shock reaches a minimum [100].

Furthermore, a large scattering may be noted between some results, as seen farther. Sometimes, these discrepancies do not permit us to correctly identify a unique relation for some parameters of the Mach disk. In what follows, we consequently propose to list the main features and the associated results expressed in function of the total pressure ratio η_0 or the exit pressure ratio η_e.

4.1.1. Position

Among the huge amount of studies, it appears that the Mach disk location is

- mainly governed by the pressure ratio [29,30,62,67–70,72,74–76,124–129,12,57,78,64,81,43,105,83–87,121,89–92,109];
- increased by the exit Mach number (for supersonic flow obtained with convergent–divergent nozzles) [29,30,68,72,78,12,83,43,105,124,128,89,90];
- independent of the fluid [67,74,78,83,43];
- not clearly influenced by the exit nozzle angle since some studies show no noticeable effects [62,68–70,74,78] while others present some influence [29,56,30,126,82,43,90], usually weak, leading to a diminution of L_{MD} with the nozzle angle β. Generally, this effect is mainly attributed to the *vena contracta* phenomenon detailed in Appendix C.
  As a final remark on this point, we will relate it to the discussion developed in Section 4.1.3 concerning the apparition of the Mach disk and the influence of the nozzle angle on the pressure ratio at which the flow switches from a regular reflection to a singular one.

Finally, in addition to the limits discussed above, we will mention that some authors observe experimentally an oscillation in the position of the Mach disk [77] and its thickness seems to increase with the pressure ratio [88]. Eventually, some numerical studies seem to underline an hysteresis in this position in function of the pressure ratio [41,130,21,115].

An exhaustive overview has been conducted on all the experimental studies available and, to compare all the results together, the measurements were non-dimensionalised by the exit diameter D_e. We present here the main conclusions, and will refer any interested reader to [131] for a complete analysis. If one first consider the results given in function of η_0 [62,67,74,64,40,81,103,84,86,87,90,92,109], we may see in Fig. 8 that the various measurements collapse on a single curve. Then it appears that relations of [67,74,64] correlate pretty well the measures. We will keep that of [74], since it was analytically obtained and validated on the largest pressure ratio range:

$$\frac{L_{MD}}{D_e} = \sqrt{\frac{\eta_0}{2.4}} = 0.645497\ \sqrt{\eta_0} \tag{5}$$

If we now consider the measurements expressed in function of η_e [29,56,30,68,69,72,75,76,126,125,12,57,78,82,83,43,105,129,121,89,91], the behavior of the position is now less clear, as shown in Fig. 9. Indeed, there seems to have no influence of the fluid (but there are too few fluids to be sure on that point) and it is not possible to find a unique relation which gives a good fit of the results, especially concerning the role of the Mach number. Finally, let us mention that the tested pressure ratio range is shorter than in the previous case, and secondly that only few measurements are available for some Mach numbers, and thirdly that discrepancies may attain 50%. Consequently, in order to separate the wheat from the chaff, using the previous result and supposing that the exit pressure ratio η_e may be computed from the total pressure ratio η_0 thanks to Eq. (68) (which corresponds to the hypothesis of a perfect gas behavior), it may be checked that relations proposed by [12,83] agree very well with Eq. (5) of [74] in the case of a sonic exit. Therefore, we propose to retain the relation of [83], because it is based on a larger set of experimental points:

$$\frac{L_{MD}}{D_e} = 0.69 M_e \sqrt{\gamma \eta_e} \tag{6}$$

Conclusion: To summarize, when we have a convergent nozzle, the best estimation of the position of the Mach disk is given by Eq. (5), namely:

$$\frac{L_{MD}}{D_e} = \sqrt{\frac{\eta_0}{2.4}} = 0.645497\ \sqrt{\eta_0} \tag{7}$$

Similar results are also obtained with Eq. (6), which also applies to convergent–divergent nozzles and consequently the Mach disk for an underexpanded jet with supersonic exit Mach numbers is located at

$$\frac{L_{MD}}{D_e} = 0.69 M_e \sqrt{\gamma \eta_e} \tag{8}$$

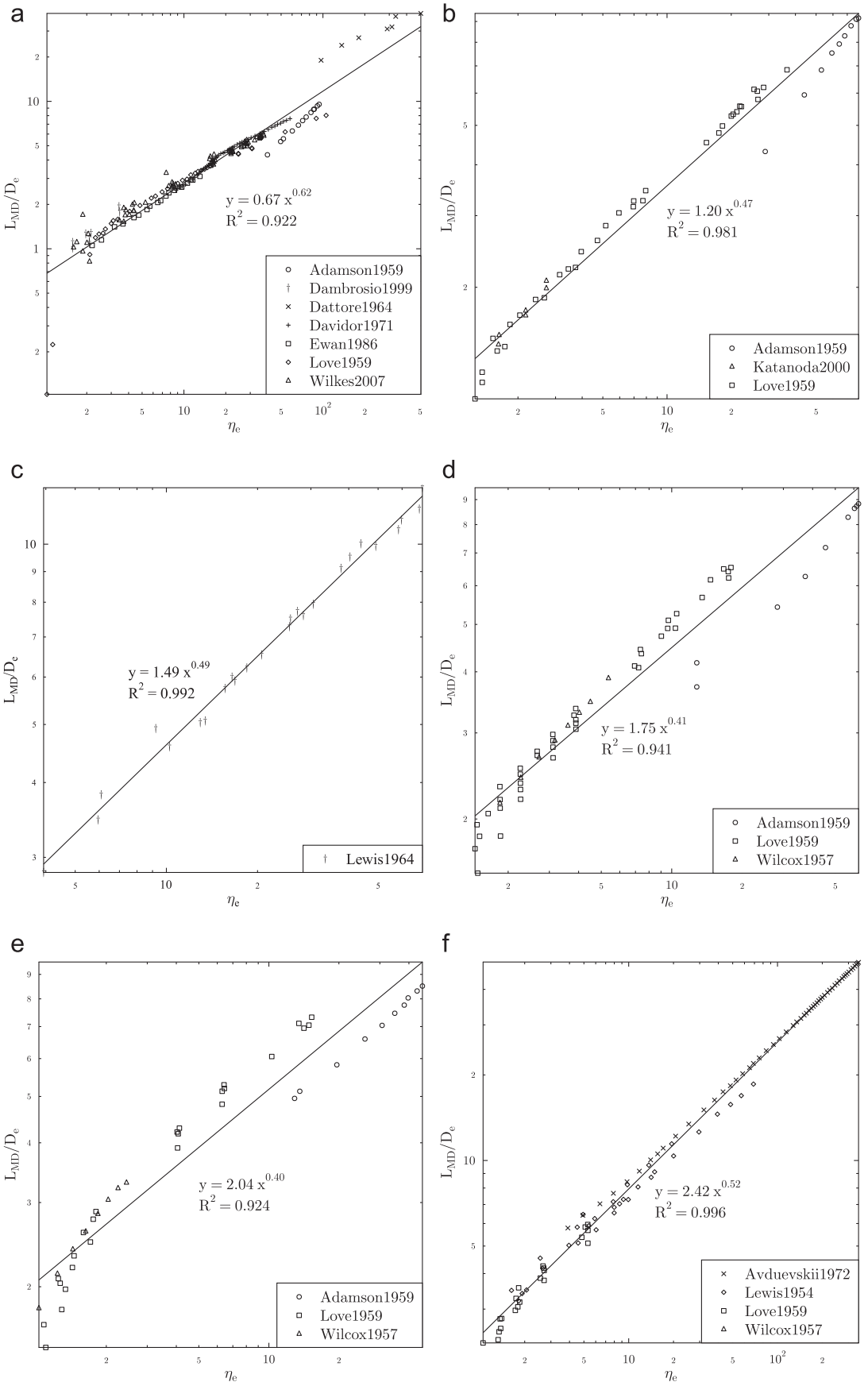

Fig. 9. Position of the Mach disk in function of the exit pressure ratio: (a) results for M_e=1.0; (b) results for M_e=1.5; (c) results for M_e=1.75; (d) results for M_e=2.0; (e) results for M_e=2.5; and (f) results for M_e=3.0.

Please cite this article as: E. Franquet, et al., Free underexpanded jets in a quiescent medium: A review, Progress in Aerospace Sciences (2015), http://dx.doi.org/10.1016/j.paerosci.2015.06.006

The influence of the nozzle angle, even small, is yet not clearly understood. Thus, one does not know if it is the same with various pressure ratios and how it quantitatively affects the position of the Mach disk.

4.1.2. Diameter

This feature has clearly been less studied than the Mach disk position, however it appears that it is

- mainly governed by the pressure ratio [62,56,30,67–69,74,81,43,124,128,14,85,129];
- apparently decreased when the exit Mach number increases [30,68,12,114,43,90], as discussed below in Section 4.1.3, yet some authors disagree with this conclusion [124,51,52];
- different for various gases [74,125,84,13] and inversely proportional to γ;
- strongly dependent on the nozzle geometry and shape [62,30,67–69,81,14]. It seems that for convergent nozzles it decreases with increasing nozzle angle [56] whereas for convergent–divergent nozzles it increases with the nozzle angle [30].

Similar to what was done in the previous section, we will present the main results and correlations, in a non-dimensionalised form, using the same methodology as above. Once more, all the corresponding results and further discussions are available in [131]. So, concerning the results in function of η_0 [62,74,64,81,84,14], presented in Fig. 10, the first remark to be done concerns the discrepancies among the measurements, particularly for the low pressure ratios. Thus, a linear function (depicted in green) could be preferably used in this range, even if the correlation is not excellent. On the contrary, for the high pressure ratios, another fitted curve (in blue) clearly shows a dependency with the square root of η_0, as suggested by [74]. Eventually, it means that one should take for the diameter of the Mach disk in function of η_0 the relations of [62] for low pressure ratios ($\gtrsim 50$):

$$\frac{D_{MD}}{D_e} = \begin{cases} 0.36\sqrt{\eta_0 - 3.9} & \text{for a contoured nozzle} \\ 0.31\sqrt{\eta_0 - 5} & \text{for a conical nozzle or an orifice} \end{cases} \quad (9)$$

and for higher pressure ratios, either the fitted curves (in black and blue) or the relation proposed by [74]:

$$\frac{D_{MD}}{L_{MD}} \longrightarrow cte \quad \text{if } \eta_0 \gg 1 \quad (10)$$

the corresponding constant being 0.6 or 0.4 for converging and straight or diverging nozzles respectively [81], which is very close to the values 0.43 and 0.57 found when using the fitted curves for the computation.

Concerning the results given in function of η_e [56,30,68,72,76,57,43,105,129,121,91], presented in Fig. 11, it is worth mentioning that pressure ratios tested are really narrower than before and, in the same time, discrepancies between the measurements are also more important. In particular, there is no obvious relation permitting us to predict the behavior in function of the exit Mach number. If only one estimation should be kept, with the previous warnings in mind, then those of [30] for low pressure ratios ($\gtrsim 100$) could be retained (although it is valid only for convergent nozzles):

$$\frac{D_{MD}}{D_e} = \frac{5}{2}\log \eta_e - \frac{3}{4} \quad (11)$$

or the one of [68] for larger ratios:

$$\frac{D_{MD}}{D_e} = A_3\left(\sqrt{\eta_e} - 1.0\right) \quad (12)$$

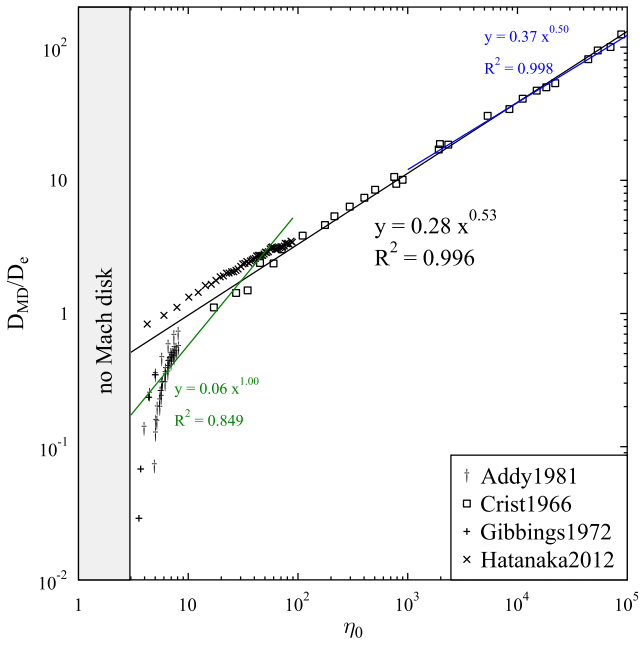

Fig. 10. Diameter of the Mach disk in function of the total pressure ratio. (For interpretation of the references to color in this figure caption, the reader is referred to the web version of this paper.)

with A_3 a constant depending on the exit Mach number, as shown in Table 1.

Conclusion: In summary, this feature is relatively well known only for convergent nozzles but there is still several candidates to represent the diameter of the Mach disk, be it Eq. (9) or (10) depending on the pressure ratio involved. Nevertheless, the role of γ is not described in these relations, although the diameter is inversely proportional to this parameter. In the case of convergent–divergent nozzles, and in particular when the exit flow is supersonic, the measurements do not permit us to retain unambiguously a relation among the available ones. Furthermore, there is no pertinent arguments to conclude on the role of the Mach number. In addition to the above-mentioned restrictions, the quantitative effects of the nozzle angle are still not well understood. Eventually, this means that there is clearly a lack of knowledge when one wants to compute the diameter of the Mach disk.

4.1.3. Apparition

Among the available papers, experimental [62,30,12,64,123,124,90], theoretical [96,29,98–100,107] or numerical [132,114,41,115], it is difficult to find quantitative results concerning the passage between regular and singular reflection. However, it seems that the boundary layer behavior and consequently the velocity field and the structure of the first cell are influenced by the shape of the nozzle (especially for CV–DV ones) [62,56,30]. Thus, it is usually admitted that the singular reflection, that is to say the apparition of a Mach disk, occurs for a wider pressure range if

- the exit Mach number increases [30,12,114,124,90,54];
- γ is increased [84,13].

Concerning the influence of the nozzle angle, it seems that it competes with the influence of the exit Mach number. Its increase leads to a larger regular reflection domain for CV nozzles [62] and to a reduction of this domain for CV–DV nozzles [30,43]. Based on these results, Antsupov [30] proposes the following relation for the limiting nozzle angle above which the Mach disk appears:

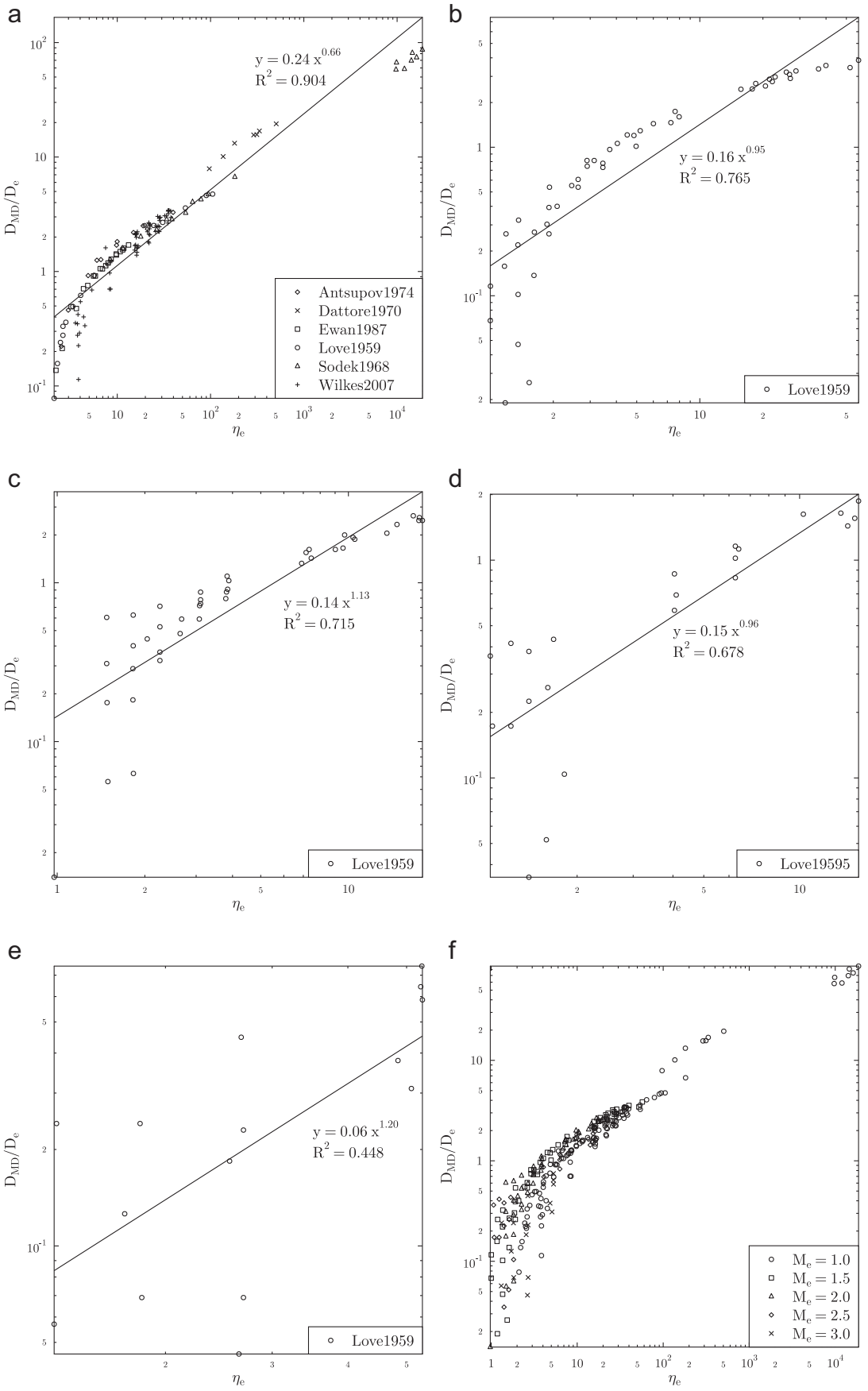

Fig. 11. Diameter of the Mach disk in function of the exit pressure ratio: (a) results for M_e=1.0; (b) results for M_e=1.5; (c) results for M_e=2.0; (d) results for M_e=2.5; (e) results for M_e=3.0; and (f) experimental results.

Please cite this article as: E. Franquet, et al., Free underexpanded jets in a quiescent medium: A review, Progress in Aerospace Sciences (2015), http://dx.doi.org/10.1016/j.paerosci.2015.06.006

Table 1
A_3 values with M_e for the diameter of the Mach disk in Eq. (12).

M_e	1	2	3	4
A_3	0.551	0.704	0.447	0.148

Table 2
Experimental studies of the nearfield zone.

Study	η_0	η_e	M_e	Species	Devices	Mach disk		Jet		
						L_{MD}	D_{MD}	θ	D	L_c
Ref. [29]		2 – 70	1 – 3	Air[a]	1 CV nozzle + 1 to 4 CV–DV nozzle	X		X		
Ref. [62]	3–9		1	Air	5 CV nozzle + 1 orifice	X	X			
Ref. [56]		2.04 and 2.56	1	Air	9 CV nozzles	X	X	X	X	
Ref. [30]		1–40	1–5.05	Air + alcohol-oxygen	1 CV nozzle + 16 CV–DV nozzles	X	X		X	X
Ref. [67]	$15–17 \cdot 10^3$		1	Air, Ar, N_2	1 CV nozzle + 1 orifice	X	X			
Ref. [68]		$1.0–4 \cdot 10^4$	1–6.0	Air[a]		X	X		X	
Ref. [70]		$1–10^4$	1–4	Air[a]		X			X	
Ref. [72]	$5–10^5$		1.0–3.0			X				
Ref. [151]		2–7	1	Air	CV nozzle					X
Ref. [74]	$10–3 \cdot 10^5$		1	N_2, Air, He, He-Ar, CO_2, Freon 22	2 CV nozzles[b]	X	X			
Ref. [35]	2–7		1	Air	CV nozzle	X				
Ref. [75]		1.59–4.53	1	Air, Ar	CV nozzle	X				X
Ref. [76]		97–506	1	burnt products	CV nozzle	X	X			
Ref. [125]		8–60	1	NO_2-N_2O_4	CV nozzle	X	X			
Ref. [12]		29–916	1–2.99	γ=1.1, 1.4, 1.67	3 CV nozzles + 2 CV–DV nozzles	X				
Ref. [39]	6.6		1	Air	CV nozzle	X				
Ref. [57]		2–15	1	Air	2 CV nozzles	X				
Ref. [78]		$10–10^4$	1–4.85	γ=1.3–1.67		X				
Ref. [79]		1–110	1	Air	slot nozzle	X				
Ref. [64]	3.52–13		1	Air	CV nozzle	X	X			
Ref. [40]	174–4067		1	N_2	CV nozzle	X				
Ref. [81]	5–90		1& 1.26	Air	3 nozzles	X	X			
Ref. [82]	4–20		1.5, 2	N_2	4 CV–DV nozzles	X				
Ref. [123]		$101–73 \cdot 10^3$	1	N_2, CO_2	CV nozzle			X		
Ref. [83]		1–100	1	N_2, CO_2, He	2 CV nozzles	X				
Ref. [43]		1–120	1–3	Air	20 CV–DV nozzles + 1 CV nozzle	X	X			X
Ref. [84]	3.6–6.4		1	moist Air	CV nozzle	X	X		X	
Ref. [85]		5–9	1	Air	CV nozzle	X	X			
Ref. [129]		$2–10^5$	1	Air	CV nozzle	X	X			
Ref. [86]	15–90		1	Air[a]	CV nozzle	X				
Ref. [87]	4–20		1	Air	2 CV nozzles	X				
Ref. [89]		2–200	1	Air	3 CV nozzles	X				
Ref. [90]	5–42		1–3.5	Air	4 CV nozzles	X				
Ref. [54]		1.6–40	1	N_2 – NO	1 CV nozzle	X	X			

[a] The fluid used is not clearly given.
[b] In fact, the number of nozzles tested is not very clear. The authors tested several exit diameters, ranging from 0.026 to 0.119 in, for a contoured and a conical nozzle.

$$\beta_{SR} = \arctan\left(0.22\sqrt{M_e - 1}\right) \tag{13}$$

4.1.4. Conclusion

To have an overall summary, it appears that the only parameter which is pretty well known, in the sense of a reliable relation giving acceptable predictions, is solely the Mach disk location. On the contrary, the corresponding diameter may be computed only in a few cases and there are still uncertainties on its expression (in particular, when one wants to identify the role of each parameter, especially the thermodynamic behavior depicted by γ). Moreover, the thickening and curving of the Mach disk are rarely considered, and almost none information is available for these features.

4.2. Spatial extension of the jet

We present here the main features of the other characteristic quantities of underexpanded jets. Here again, the interested reader is referred to [131] for the complete set of data and related discussions.

4.2.1. Initial divergence angle

As the gas emerges from the device, it is known to undergo a Prandtl–Meyer expansion. In the general case, the angle taken by the jet depends on the nozzle angle and on the Prandtl–Meyer angle, which one is dependent on the ambient Mach number and the exit Mach number (and consequently on the pressure ratio). Moreover, it appears that the nozzle geometry may modify the initial jet angle [56,133,117,118,128,14,129,53]. Eventually, the thermodynamical behavior of the fluid may also play a significant role since the angle is inversely proportional to γ [74,43,53] and real gas effects increase the jet divergence [129].

4.2.2. Diameter

When considering this feature, one has to pay attention because it may be related either to the plume jet boundary or to the intercepting shock. Therefore, both characteristics are studied separately henceforth.

Diameter of the jet: This feature is not easily studied, and consequently it is uneasy to find quantitative results among the few

Table 3
Evolution of the variables in the nearfield zone.

Study	Work	Axial evolution					Radial evolution				
		Velocity	Mach	Pressure	Density	Concentration	Velocity	Mach	Pressure	Density	Concentration
Ref. [191]	Num.–Exp.	X	X	X				X	X		
Ref. [110]	Num.		X	X							
Ref. [66]	Exp.	X					X				
Ref. [144]	Exp.			X							
Ref. [145]	Exp.			X							
Ref. [30]	Exp.			X							
Ref. [157]	Exp.								X		
Ref. [67]	Exp.			X					X		
Ref. [70]	Exp.			X					X		
Ref. [32]	Exp.							X	X		
Ref. [132]	Num.			X							
Ref. [134]	Num.–Exp.				X					X	
Ref. [135]	Exp.				X	X				X	X
Ref. [63]	Num.		X								
Ref. [192]	Num.–Exp.								X		
Ref. [138]	Num.			X							
Ref. [111]	Num.			X	X						
Ref. [147]	Num.	X		X				X			
Ref. [148]	Num.–Exp.	X		X		X	X				
Ref. [151]	Exp.			X							
Ref. [268]	Num.	X		X		X		X			
Ref. [34]	Num.	X				X	X				
Ref. [35]	Exp.				X						
Ref. [75]	Num.–Exp.	X			X						
Ref. [175]	Num.						X				
Ref. [112]	Num.			X							
Ref. [176]	Num.		X	X					X		
Ref. [215]	Num.			X							
Ref. [193]	Exp.					X					
Ref. [77]	Exp.	X	X	X							
Ref. [38]	Exp.	X									
Ref. [113]	Num.		X	X							
Ref. [39]	Exp.	X					X				
Ref. [15]	Exp.									X	
Ref. [216]	Num.	X	X	X			X	X			
Ref. [195]	Exp.			X							
Ref. [64]	Exp.							X	X		
Ref. [142]	Exp.			X							
Ref. [217]	Num.			X							
Ref. [156]	Exp.		X								
Ref. [115]	Num.			X							
Ref. [218]	Num.		X	X					X		
Ref. [288]	Exp.				X					X	
Ref. [82]	Exp.			X							
Ref. [159]	Exp.				X						
Ref. [199]	Exp.				X					X	
Ref. [123]	Exp.				X						
Ref. [200]	Exp.	X									
Ref. [201]	Exp.				X					X	
Ref. [42]	Exp.				X						
Ref. [116]	Num.	X					X				
Ref. [127]	Exp.				X					X	
Ref. [103]	Exp.				X						
Ref. [202]	Exp.			X					X		
Ref. [289]	Exp.		X		X						
Ref. [205]	Num.–Exp.	X	X	X	X					X	
Ref. [163]	Exp.									X	
Ref. [152]	Exp.									X	
Ref. [221]	Num.	X		X							
Ref. [14]	Num.			X							
Ref. [21]	Num.			X							
Ref. [210]	Exp.			X							
Ref. [222]	Num.		X								
Ref. [164]	Exp.		X								
Ref. [184]	Exp.		X		X					X	
Ref. [143]	Exp.			X							
Ref. [120]	Num.	X									
Ref. [55]	Num.	X					X				
Ref. [149]	Exp.			X							
Ref. [51]	Exp.		X	X				X	X		
Ref. [52]	Exp.		X	X							
Ref. [87]	Exp.				X						
Ref. [121]	Num.	X	X	X	X		X	X			X

Please cite this article as: E. Franquet, et al., Free underexpanded jets in a quiescent medium: A review, Progress in Aerospace Sciences (2015), http://dx.doi.org/10.1016/j.paerosci.2015.06.006

Table 3 (*continued*)

Study	Work	Axial evolution					Radial evolution				
		Velocity	Mach	Pressure	Density	Concentration	Velocity	Mach	Pressure	Density	Concentration
Ref. [223]	Num.		X	X							
Ref. [272]	Num.	X					X				
Ref. [206]	Exp.			X	X						
Ref. [122]	Num.–Exp.		X	X	X				X		
Ref. [150]	Exp.		X								

Table 4
Experimental studies of the farfield zone.

Study	η_0	η_e	Jet[a]	Devices	Species	Measurements[b]	
						Concentration	Velocity
Ref. [224]	2–70		V	Nozzle	NG[c], C_2H_4	X (A)	
Ref. [225]	2–75		V	Nozzle	Air		X (A)
Ref. [226]	100		H	Orifice	H_2, CH_4	X (A)	
Ref. [57]	5.7–20		H	Nozzle	Air, *He*		X (A)
Ref. [244]	100		H	Nozzle	H_2	X (A)	
Ref. [251]							
Ref. [290]	20–260		H	Nozzle	H_2	X (A)	X (A,R)
Ref. [291]		200–400	H	Orifice	H_2	X (A)	
Ref. [292]		5–25	H	Orifice	H_2	X (A)	
Ref. [230]	52–163		H	Nozzle	H_2	X (A)	X (A)
Ref. [231]	40		H	Nozzle	CH_4, H_2	X (R)	X (A,R)
Ref. [247]	5–60		H	Nozzle	H_2	X (R)	X (A,R)
Ref. [248]	17–68.5		H	Orifice	H_2	X (A)	X (A,R)
Ref. [207]		1–20.3	H	Nozzle	Air		X (A,R)

[a] Horizontal (H) or vertical (V).
[b] Axial (A) or radial (R).
[c] Natural gas with 92–92.4% of CH_4.

theoretical [29,30,133–136,99,76,100,43,128,46,53] and experimental [64] and numerical papers [137,138,112,117,118,84,14] thereon. To summarize, it is common to describe both the diameter of the jet and its maximum value for which it appears that

- both increase with the pressure ratio [30,68,69,65,43,85,129,53] until a priori an asymptotic value [30,43];
- they seem to increase with the exit Mach number [68,43,85] even if some authors disagree on that point [30];
- they increase with the nozzle angle [68,70,43,85];
- they are inversely proportional to γ [30,74,43,85];
- they are inversely proportional to the density ratio [134,135].

From a practical point of view, there are not so many data permitting us to quantitatively describe this feature, essentially because it was not so easy to clearly measure it. Thus, let us note that only Antsupov [30] proposes a relation (for CV–DV nozzles and for $\eta_e \leq 40$):

$$\max\left(\frac{D_{\text{jet}}}{D_e}\right) = \left(1 + 0.57\theta_e\right)\eta_e^{0.6} \tag{14}$$

Diameter of the intercepting shock: More studies have been dedicated to this feature, both experimentally [56,69–71,123], theoretically [69,70,72,99,76,139,100,102,140,105,128,107] and numerically [141,137,138,112,117,118,84]. Surprisingly enough, the available data are quite poor and one may only say that it

- seems to be also dependent on the square root of the pressure ratio [69,70,123];
- may sometimes depend on the convergence angle [68,70,117] even if it is not the case for some configurations [56,70].

As before, if all the useful papers are analyzed [56,68,72,123], it may be seen in Fig. 12 that no argument emerges to discriminate

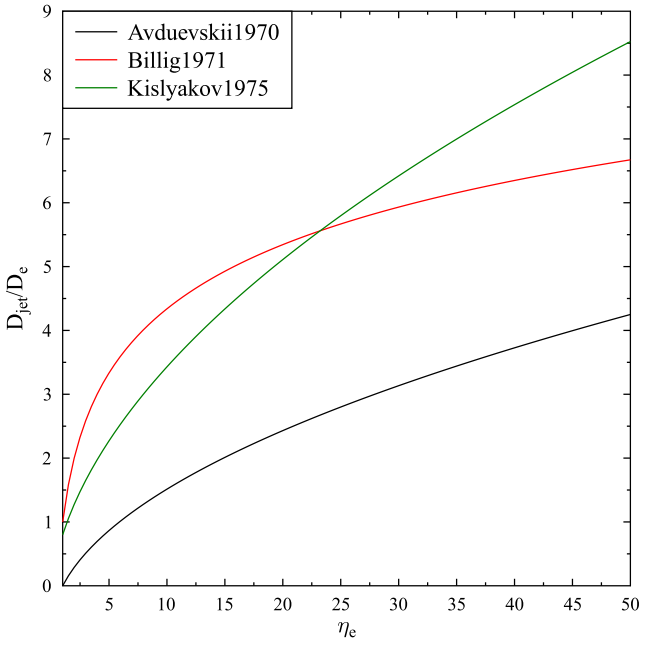

Fig. 12. Maximum value for the diameter of the intercepting shock in function of the exit pressure ratio.

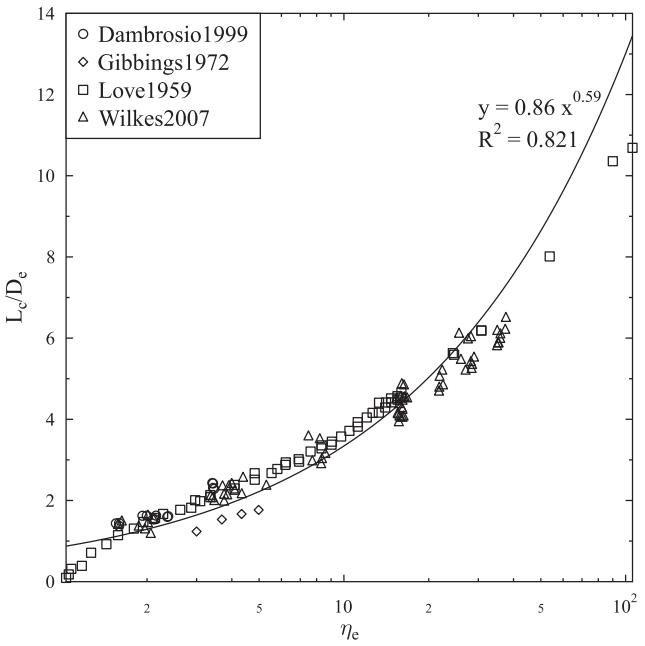

Fig. 13. Length of the first cell in function of the exit pressure ratio (CV nozzle).

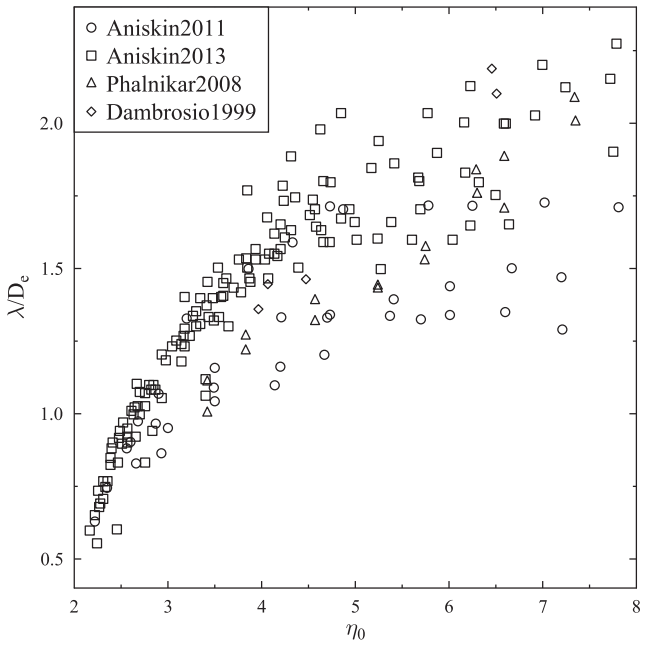

Fig. 14. Wavelength in function of the total pressure ratio.

the relations altogether, which are although very different.

Conclusion: Globally, there is a lack of data concerning this feature. Even if the dependency with the square root of the pressure ratio seems reasonable, it is not clearly proven. Moreover, there is a large scatter of the quantitative results since computations with the various expressions available evidence a discrepancy of up to 50%.

4.2.3. Length of the first cell

This feature is also poorly documented and there are still few papers that give some insights on this characteristic length, be it experimentally [56,30,75,64,43,91], theoretically [101,142,46,47,7] or numerically [75,112,119,91]. The main reason is certainly the various issues raised by its observation. However, the following properties for the length of the first cell may be retained:

- it increases with the pressure ratio [30,75,64,43,47,121];
- it increases with the exit Mach number [30,43,46,121];
- it depends on the geometry of the nozzle [56,30,43,51].

From a quantitative point of view, the concerned papers [56,30,75,64,43,47,91] only permit us to consider the case of converging nozzles. Indeed, only the measurements of [43] are concerned with supersonic exit Mach numbers. Consequently, keeping only the sonic cases, a fitted curve may be computed, as shown in Fig. 13, yet the relation is not very good. If only one estimation is to be taken, then we propose to keep the empiric estimation of [43] (even if the authors agree themselves that it seems to overestimate the cell length):

$$\frac{L_{\text{¢}}}{D_e} = 1.52\,\eta_e^{0.437} + 1.55\left(\sqrt{2M_e^2 - 1} - 1\right) - 0.55\sqrt{M_e^2 - 1} + 0.5\left(\frac{1}{1.55}\sqrt{\left(\eta_e - 2\right)\sqrt{M_e^2 - 1}} - 1\right) \tag{15}$$

4.2.4. Wavelength of the cell structures

Once more, the behavior of the cell structures is badly known, be it their exact number or the distance between each Mach disks in the case of multiple cells, mainly because the flow is not stationary on average anymore. Therefore, it is hard to determine exactly the position of each shock. Although quantitative studies are solely encountered, the number of structures is known to depend on:

- the pressure ratio [5,43,47,143,51,54];
- the exit Mach number [143,51].

First, let us recall that it is not straightforward to compare measurements obtained either with convergent nozzles or with convergent–divergent ones. This implicitly raises the question of the relation between each quantitative results given hereafter. Furthermore, to the best of our knowledge, there are only a few quantitative measurements and consequently the degree of confidence is not very high. If, as usual, all these measurements [143–146,75,5] are compared altogether, which is done in Fig. 14, it is straightforward to note that large discrepancies (up to 100%) exist between the different measurements. Similarly, no expression seems to be better than the other ones however the one of [143] seems to be the most representative of the experimental results:

$$\frac{\lambda}{D_e} = 0.57M_{\text{id}}^2 - 0.15 \tag{16}$$

4.2.5. Length of the potential core

Usually, it is admitted that the nearfield zone ends at the point where the mixing layers around the potential core merge together on the centerline of the jet. The corresponding distance from the nozzle is

- greater for compressible jets and particularly for the ones that are not ideally expanded [147–150,108,51,121];
- increased for larger pressure ratios [143–145,149,121,150];
- increased with the exit Mach number [149];
- reduced when there occurs an enhancement of the turbulence, and so depends on the Reynolds number, which induces a rapid mixing of the high-velocity flows with the ambient fluid since we may have a thicker shear layer [144,148,151–154,38,61].

Unfortunately, the only available quantitative results mainly deal with the supersonic core length [143–145,149], which differs

Please cite this article as: E. Franquet, et al., Free underexpanded jets in a quiescent medium: A review, Progress in Aerospace Sciences (2015), http://dx.doi.org/10.1016/j.paerosci.2015.06.006

from the length we are interested in since this one may be shorter than the supersonic one that may penetrate in the farfield zone [28,155]. Thus, the only papers providing quantitative results for the length of the potential core [30,156] show a tendency which reads

$$L_{NZ} = L_{RR} + 4\lambda \tag{17}$$

Then, when one turns to the supersonic core length, the only available relation (obtained for converging micro-nozzles) is furnished by [143]

$$\frac{L_s}{D_e} = 1.81\eta_0 + 2.98 \tag{18}$$

4.2.6. Mixing layer

A huge amount of papers have been devoted to the understanding and analysis of the main features of the mixing layer, which is shown to contain large-scale eddies (described in detail hereafter). Most of these studies are experimental ones [30,65,59,135,157–174,149,122,61,94] yet some numerical papers are also available [37,59,122,175–181]. These structures play a major and significant role in the behavior of the jet, especially in its spreading rate and the associated decay, because of their interaction with the various shock waves [134,38,158,156,164,52,149,178,166,171]. Contrary to what happens in the core of the jet, the viscous effects have here a tremendous influence, particularly because of their impact on the development of the flow instabilities and consequently on the width of the mixing layer and on the diameter of the jet. This has been formalized by [69], and confirmed by [163,152,162], who defined an initial Reynolds number Re_i for the shear layer, based on the exit velocity and the distance to the Mach disk and the viscosity of the ambient fluid, such that for

- $Re_i > 10^4$, the mixing layer is initially turbulent and its width increases linearly with the distance to the exit plane, leading to the replication of identical shocks pattern whose characteristic lengths are governed by the pressure ratio.
  Let us note here that this case is the most often encountered in practical situations.
- $10^3 < Re_i < 10^4$, the regime is essentially laminar but the transition to turbulence occurs before the Mach disk, the corresponding transition point being closer to the exit plane as Re_i increases, accompanied by a progressive decrease of the diameter of the suspended shock and a thickening of the mixing layer.
- $10^2 < Re_i < 10^3$, the flow is laminar in the mixing layer, whose width increases with Re_i, and the shock waves pattern may be greatly modified (in particular the intercepting shock).
- $Re_i < 10^2$, the flow behaves as in a rarefied regime and the shocks are extremely diffuse.

Hydrodynamic instabilities: Two kind of flow instabilities may be found in the mixing layer: Kelvin–Helmholttz (KH) instability and Taylor–Goertler (TG) instability. The first one arises because there is a great shearing between the various streamlines present in the mixing layer. Indeed, as we have seen previously, the flow has a great velocity in the core part and passes from a supersonic regime to a subsonic regime since the ambient fluid is at rest. A shear layer is present between the intercepting shock and the frontier of the jet, which permits the appearance of KH type instabilities. These ones appear as roll-ups and become large eddies, producing vortex rings which evolve downstream of the flow, mainly by entrainment of the ambient fluid [59,177,182,183]. Their amplitude evolution may become non-linear. Concerning the TG instability, this is caused by the curvature of the streamlines in the mixing layer. This curvature is mainly due to the high expansion of the fluid (the greater the expansion – the pressure ratio – the stronger the curvature) but it depends also on the exit Mach number and on the boundary layer of the jet inside the device which undergoes the under expansion [170,172,174,180,181]. Consequently, the fluid moves along curvilinear trajectories and is influenced by centrifugal forces proportional to the square of the velocity and to the inverse of the radius of curvature [179,174]. This, combined with the strong radial velocity gradient, induces the development of non-uniformities in the flow, eventually taking the form of pairs of counter-rotating vortices with axis parallel to the centerline, which are stationary (or quasi-stationary). Their size is of the order of the boundary-layer thickness but increases downstream and with the pressure ratio [157,152,179,165,166,181]. Furthermore, these disturbances tend to amplify initial perturbations due to the nozzle boundary layer or to some features of the nozzle walls, such as the roughness of their inner side that can be connected to the streamwise vortex structures [151,160,162,152,167,169].

Influence on the flow behavior: The previous instabilities strongly affect the flow since the shock waves pattern is perturbed, which is the first reason for the unsteady behavior of the jet. Thus, when the eddies are convected they finally encounter an oblique shock, leading to the emission of acoustic waves which may move upstream and perturb the jet boundary and structure back to the nozzle exit. This logically induces a feedback loop, whose coupling will depend on the pressure ratio [59,164,184]. Furthermore, the counter-rotating vortices modify the azimuthal distributions of the characteristic variables, which appear to have a petal-like structure. Hence, one may observe local maxima and minima exhibiting sinuous type variation, whose spatially modulated magnitude increases with the distance from the exit plane as the eddies grow in size [30,157,65,152,167,94,171,174,181]. Apparently, the maxima of density and of convective speed coincide together [184]. Eventually, these vortices play a significant role in the jet noise related mechanisms. Indeed, it seems that the vortex pairs are the origin of Mach-waves which are the most dangerous part of the noise [182,183,185]. This topic is nonetheless beyond the scope of the present paper, and therefore we will refer the interested reader to some of the basic studies dedicated to this issue [146,185–190,182,183].

Conclusion: Eventually, the phenomena arising inside the mixing layer are pretty well understood. Nevertheless, there are still some unknowns concerning the quantitative influence of the interaction between the hydrodynamic instabilities and the shock waves structure of the jet. In the same way, the role of the ambient conditions (especially the density) is ill-known. Last but not least, the structure of the turbulence, its morphology and its dynamics, still needs some additional thorough investigations regarding the distance for the turbulent transition or the anisotropy of the turbulence field.

4.3. Evolution of the flow variables

Many studies have tried to determinate the evolution of the variables during the expansion and recompression process as far as the fluid emerges outside the confining device. Thus, one may easily find experimental works [66,144,145,30–32,157,70,134,135,191–207,148,151,35,77,38,39,15,64,40,142,82,123,159,42,127,59,55,51,87,60,122,150], as well as theoretical ones [133,74,75,38,78,142,159,127,103,13,208–211,108,129,178,181] or numerical papers [191,110–117,212–223,31,132,63,192,138,147,148,34,37,196,40,41,82,205,59,119,14,184,120,55,121,122] which provide axial variation (usually along the centerline) of some variables or sometimes the radial evolution at different positions along the centerline. An overview of the various results is given in Table 3.

Please cite this article as: E. Franquet, et al., Free underexpanded jets in a quiescent medium: A review, Progress in Aerospace Sciences (2015), http://dx.doi.org/10.1016/j.paerosci.2015.06.006

5. Farfield zone of a highly underexpanded jet

In comparison with the nearfield zone, this region has focused less attention in the past (excluding obviously the ideally expanded jets) however some information may be found concerning the behavior of the jet characteristics since both experimental [30,70,148,39,57,224–232,61,207] and theoretical [28,72,224–226,197,228,233–241,207] and numerical [34,216,230,242–249,238] papers report thereon. Generally, they deal with risk assessment related to leakage of flammable material (e.g. natural gas or hydrogen). As previously explained (see Section 3.3), the jet is now in pressure equilibrium with the ambient fluid although it may still have a high velocity (i.e. evolve in the compressible regime) which decays farther downstream. In this context, it has been shown that the behavior of underexpanded jets may be treated as usual compressible fully expanded jets, provided that suitable arrangements are done in order to find a characteristic length which permits us to scale all the variables of the jet [28,68,70,224,243,38,197,150]. Thus, as depicted in Fig. 15, one may view the jet in this region as if it were originated from a pseudo-source with different characteristics than the actual exit source. When dealing with practical applications, the aim is thus to feed industrial codes with proper boundary conditions in order to avoid the resolution of the whole underexpanded jet which would be cumbersome (and still very complicated even at the present time). We present hereafter how this pseudo-source, often referred to as a notional nozzle, may be described (Fig. 16).

5.1. Notional or fictional or equivalent nozzle

Far downstream from the exit plane, the jet seems to have little memory of its recent past (the shock wave pattern, the presence of multiple or a unique Mach disk, etc.). From this observation, it has long been proposed to replace it by an equivalent flow, whose characteristics are determined only from stagnation (or exit) state thanks to some simple physical hypotheses. Let us now present the available models, in the case of a chocked convergent nozzle such that the flow is sonic at the exit.

5.1.1. Equivalent diameter [250]

This paper related to reactive jets studies the dimensionless parameters governing the flame length when there are changes of jet momentum, and also an excess air ratio. It is generally renowned as the first study introducing the concept of an equivalent diameter (or nozzle), in order to take into account the density effects in the axial decay of jets. This equivalent nozzle is supposed to have the same momentum flux and velocity as the actual nozzle but with the density of the ambient fluid. Then, without the help of any hypothesis on the equation of state, conservation equations for the nozzle fluid mass and momentum lead to the following equivalent diameter:

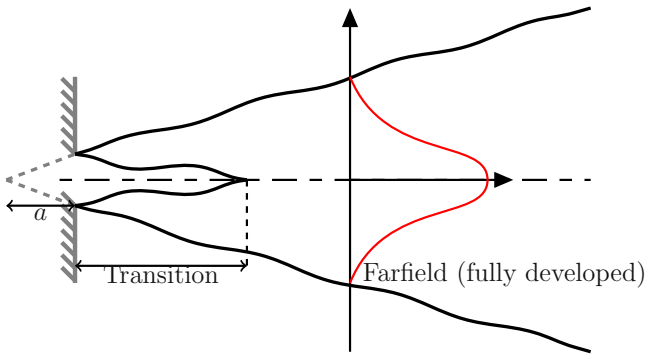

Fig. 15. Flow behavior in the farfield zone and notional nozzle concept.

$$\frac{D_{eq}}{D_e} = \sqrt{\frac{\rho_e}{\rho_\infty}} \tag{19}$$

Obviously, for a perfect gas, we may use Eq. (70) to rewrite this relation:

$$\frac{D_{eq}}{D_e} = \sqrt{\left(\frac{2}{\gamma+1}\right)^{1/(\gamma-1)} \frac{\rho_0}{\rho_\infty}} = \sqrt{\left(\frac{2}{\gamma+1}\right)^{1/(\gamma-1)} \frac{T_\infty}{T_0}\,\eta_0} \tag{20}$$

5.1.2. Pseudo-diameter approach [224]

It relies on the mass conservation, assuming no entrainment of ambient air, between the exit plane to an hypothetical state in the farfield zone where the flow is supposed to be at the same pressure and temperature as the ambient fluid and at a sonic velocity. This may be summarized as follows:

$$p_{eq} = p_\infty \tag{21}$$

$$T_{eq} = T_\infty \tag{22}$$

$$V_{eq} = c_{eq} \tag{23}$$

From the mass balance, we may obtain

$$\frac{D_{eq}}{D_e} = \sqrt{\frac{\rho_e V_e}{\rho_{eq} c_{eq}}} \tag{24}$$

For a fluid governed by the perfect gas equation of state, Eqs. (68) and (69) may be used to rewrite the mass balance as follows:

$$\frac{D_{eq}}{D_e} = \sqrt{\left(\frac{2}{\gamma+1}\right)^{\gamma+1/2(\gamma-1)} \eta_0 \sqrt{\frac{T_\infty}{T_0}}} \tag{25}$$

Remark: in the two previous relations, we voluntary omitted the discharge coefficient present in the original paper in order to have the same basis when comparing the various results.

5.1.3. Sonic jet approach [57]

This method is almost the same as the pseudo-diameter approach [224], since it also relies on the mass conservation and supposes that the equivalent flow is sonic at the ambient pressure but at the same temperature as in the exit plane. This summarizes as follows:

$$p_{eq} = p_\infty \tag{26}$$

$$T_{eq} = T_e \tag{27}$$

$$V_{eq} = c_{eq} \tag{28}$$

The effective diameter is then easily found, namely:

$$\frac{D_{eq}}{D_e} = \sqrt{\frac{\rho_e V_e}{\rho_{eq} c_{eq}}} \tag{29}$$

For a fluid governed by the perfect gas equation of state, Eq. (29) may be written:

$$\frac{D_{eq}}{D_e} = \sqrt{\eta_e} = \sqrt{\left(\frac{2}{\gamma+1}\right)^{\gamma/(\gamma-1)} \eta_0} \tag{30}$$

5.1.4. Momentum-velocity approach [227]

In this method, the diameter of the jet is not modified but an equivalent velocity is computed so as to preserve the momentum balance, leading to the following relations:

Please cite this article as: E. Franquet, et al., Free underexpanded jets in a quiescent medium: A review, Progress in Aerospace Sciences (2015), http://dx.doi.org/10.1016/j.paerosci.2015.06.006

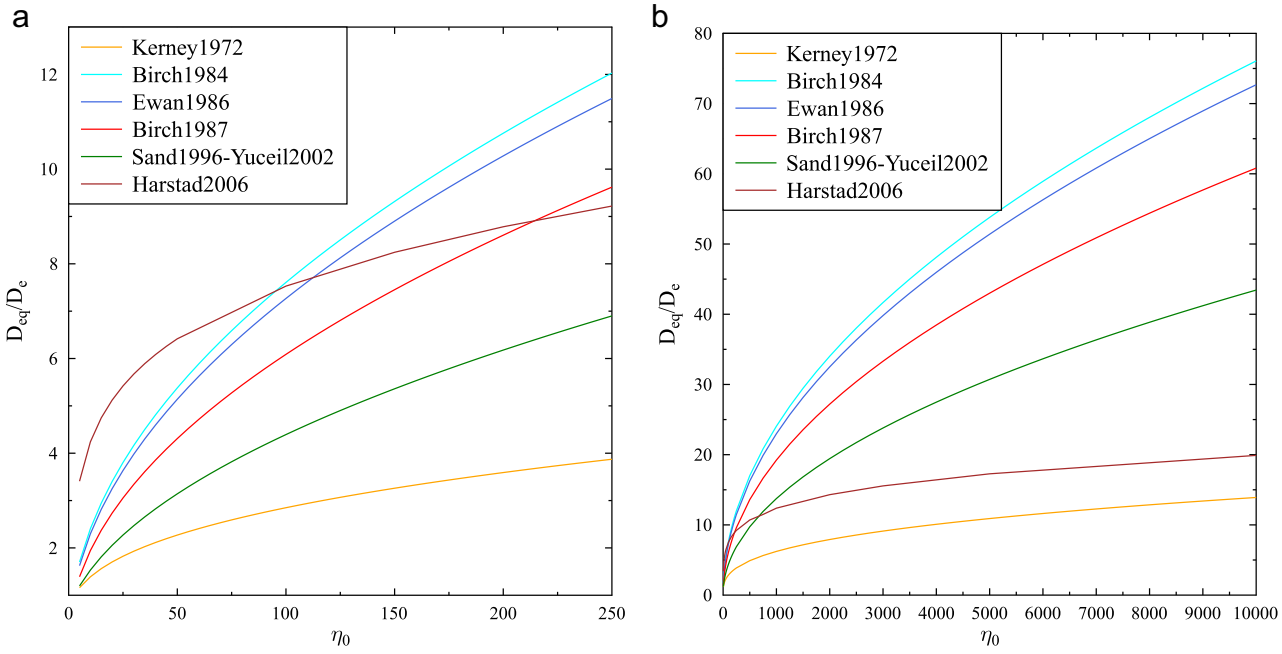

Fig. 16. Effective diameter of the equivalent jet in function of the total pressure ratio: (a) low pressure ratios and (b) high pressure ratios.

$$V_{eq} = V_e + \frac{p_e - p_{eq}}{\rho_e V_e} \tag{31}$$

$$\frac{D_{eq}}{D_e} = 1 \tag{32}$$

5.1.5. Improved pseudo-diameter approach [225]

It is an extension of the method developed in [224], and previously given in Section 5.1.2, where both mass and momentum balances are used. The flow is still supposed to be in pressure equilibrium with the ambient medium but its temperature is equal to the total one:

$$p_{eq} = p_\infty \tag{33}$$

$$T_{eq} = T_0 \tag{34}$$

By combining the mass and momentum equation, one may have

$$V_{eq} = V_e + \frac{p_e - p_\infty}{\rho_e V_e} \tag{35}$$

Consequently, the diameter is easily deduced via the mass balance:

$$\frac{D_{eq}}{D_e} = \sqrt{\frac{\rho_e V_e}{\rho_{eq} V_{eq}}} \tag{36}$$

These relations are valid for any kind of equation of state, nevertheless in the case of a perfect gas, we may write them:

$$V_{eq} = c_e \frac{\gamma + 1 - \frac{\eta^\star}{\eta_0}}{\gamma} \tag{37}$$

$$\frac{D_{eq}}{D_e} = \sqrt{\left(\frac{2}{\gamma+1}\right)^{1/(\gamma-1)} \frac{\gamma\,\eta_0}{1 + \gamma - \frac{\eta^\star}{\eta_0}}} \tag{38}$$

When the pressure ratio is far from its critical value ($\eta_0 \gg \eta^\star$), Eq. (38) becomes

$$\frac{D_{eq}}{D_e} = \sqrt{\frac{\gamma}{\gamma+1}\left(\frac{2}{\gamma+1}\right)^{1/(\gamma-1)} \eta_0} \tag{39}$$

Remark: here again, we do not put the discharge coefficient in the previous relations contrary to what is done in the associated paper.

5.1.6. Adiabatic expansion approach [238,207,248]

This method has been tried first in [238] and completely presented in [207]. Contrary to others methods, it considers a complete conservative approach which therefore includes the mass, momentum and energy balances. Supposing that body forces, entrainment and viscous forces are negligible, a quasi-steady expansion up to the ambient pressure is assumed, namely:

$$p_{eq} = p_\infty \tag{40}$$

With such an approach, not only the effective diameter of the equivalent jet is calculated but also its velocity, enthalpy and density. Thus, we have

$$\frac{V_{eq}}{V_e} = 1 + \frac{1}{\gamma M_e^2} \frac{\eta_e - 1}{\eta_e} \tag{41}$$

$$\frac{h_{eq}}{h_e} = 1 + \frac{1}{2} \frac{M_e^2 c_e^2}{h_e} \left(1 - \left(\frac{V_{eq}}{V_e}\right)^2\right) \tag{42}$$

$$\frac{\rho_{eq}}{\rho_e} = \frac{\rho(p_{eq}, T_{eq})}{\rho(p_e, T_e)} \tag{43}$$

$$\frac{D_{eq}}{D_e} = \sqrt{\frac{\rho_e V_e}{\rho_{eq} V_{eq}}} \tag{44}$$

For a perfect gas, these relations may be analytically developed:

$$\frac{T_{eq}}{T_e} = 1 + \frac{\gamma - 1}{2} M_e^2 \left(1 - \left(\frac{V_{eq}}{V_e}\right)^2\right) \tag{45}$$

$$\frac{\rho_{eq}}{\rho_e} = \frac{1}{\eta_e} \frac{T_e}{T_{eq}} \tag{46}$$

5.1.7. Mach disk approach [197,241]

The notional nozzle is supposed to be positioned just after the Mach disk, whose diameter will be taken as the one of the equivalent jet. Supposing that the flow undergoes an isentropic expansion up to the Mach disk, considered as a normal shock wave, and assuming a post-shock pressure equal to the ambient one, it is possible to combine the isentropic and normal shock relations to obtain an equation whose solution provides the Mach number upstream of the Mach disk. Knowing this latter one, the equivalent diameter is computed from the exit diameter.

In the case of a perfect gas equation of state, the combination of Eq. (60) and (74) yields to the equation giving the Mach number before the Mach disk, which permits us to compute the equivalent diameter thanks to Eq. (67). This summarizes as follows:

$$\eta_0 = \frac{\left(1 + \frac{\gamma - 1}{2} M^2\right)^{\gamma/(\gamma-1)}}{\frac{2\gamma}{\gamma + 1}\left(M^2 - 1\right) + 1} \tag{47}$$

$$\frac{D_{eq}}{D_e} = \frac{1}{M}\left(\frac{1 + \frac{\gamma - 1}{2} M^2}{\frac{\gamma + 1}{2}}\right)^{\gamma + 1/4(\gamma-1)} \tag{48}$$

5.1.8. Underexpanded jet theory [251]

It is principally based on mass and energy conservations, with the assumption of no ambient fluid entrainment. Similar to most existing approaches, the notional nozzle is supposed to be sonic and the fluid in pressure equilibrium with the ambient fluid:

$$p_{eq} = p_\infty \tag{49}$$

$$V_{eq} = c_{eq} \tag{50}$$

The equivalent diameter is still computed from the mass balance:

$$\frac{D_{eq}}{D_e} = \sqrt{\frac{\rho_e V_e}{\rho_{eq}\, c_{eq}}} \tag{51}$$

with $\rho_{eq} = \rho(p_\infty, T_{eq})$ and $c_{eq} = c(p_\infty, T_{eq})$. Here, the temperature is obtained via the energy balance:

$$h_0 = h_{eq} + \frac{V_{eq}^2}{2} \tag{52}$$

As previously, these relations are easily obtained for a perfect gas:

$$T_{eq} = \frac{2}{\gamma + 1} T_0 \tag{53}$$

$$\frac{D_{eq}}{D_e} = \sqrt{\eta_e} = \sqrt{\left(\frac{2}{\gamma + 1}\right)^{\gamma/(\gamma-1)} \eta_0} \tag{54}$$

Remark: in such a case, one may note that this leads to the same expression as with the sonic jet approach of [57] since we obtain $T_{eq} = T_e$.

5.1.9. Comparison of the various approaches

Given the previous methods to estimate the diameter of the equivalent jet, we propose to compare them altogether, with the exception of the approximation of Thring and Newby [250] which systematically leads to higher values and disagrees with all other relations [131]. Yet, concerning the other methods, the discrepancies between the results lie between 67% and 80% depending on the pressure ratio. Since the notional nozzle may represent a hypothetical state, which does not exist physically, it is not possible to discriminate the various approaches. Consequently, we are going to further study the predictions that can be done using such models.

5.2. Evolution of the variables

Since the flow has a gaussian profile in this region, most of the experimental works, whose conditions and main results are detailed in Table 4, deal with the axial evolution of some physical variables, which ones are commonly the velocity and the concentration (based either on the volume fraction or on the mass fraction). Given these measurements, we are now going to present how the previous models may be used to obtain a quantitative description of the jet. From a general point of view, there are two classical ways to handle the difficulty to model in a simple manner the evolution of the variables along the centerline. The first one relies on the extension of the work of [252] who studied ideally expanded supersonic jets and proposed the following expression for the evolution of any unknown variable U such as the velocity, the mass fraction or the stagnation enthalpy:

$$\frac{U}{U_e} = 1 - \exp\left(-\frac{1}{\zeta \frac{x}{D_e}\sqrt{\frac{\rho_\infty}{\rho_{eq}}} + a}\right) \tag{55}$$

with $\zeta = 0.037$, 0.052 or 0.051 and $a = -0.7$ respectively.

Concerning the decay of the velocity, one may also find the following expressions:
Ref. [253]:

$$\zeta = 0.16(1 - 0.16 M_{id}) \tag{56}$$

Ref [153,154]:

$$\zeta = \begin{cases} 0.16\left(1 - 0.16 M_{id}\right)\left(\frac{\rho_\infty}{\rho_e}\right)^{-0.22} & \text{for } M_{id} \le 0.81 \\ 0.126\left(M_{id}^2 - 1\right)^{-0.15} & \text{for } M_{id} \ge 1 \end{cases} \tag{57}$$

The second method, far more famous, proposes to extend the use of the classical relation of [254] based on the observations of [250]. This one, developed for subsonic jets, states that the axial evolution of the mass fraction and velocity are given by

$$\frac{U}{U_e} = \kappa \frac{D_e}{x + a}\sqrt{\frac{\rho_{eq}}{\rho_\infty}} \tag{58}$$

with $\kappa = 5 - 5.4$ or $5.8 - 6.2$ for each variable.

Here, it is interesting to remark that far away from the exit, the denominator in the exponential term of Eq. (55) is huge and consequently this relation may be rewritten as

$$\frac{U}{U_e} = \frac{1}{\zeta}\frac{D_e}{x}\sqrt{\frac{\rho_{eq}}{\rho_\infty}} \tag{59}$$

Practically, this means that in the farfield, the expression of [252] is equivalent to the hyperbolic decay proposed in [254].

Please cite this article as: E. Franquet, et al., Free underexpanded jets in a quiescent medium: A review, Progress in Aerospace Sciences (2015), http://dx.doi.org/10.1016/j.paerosci.2015.06.006

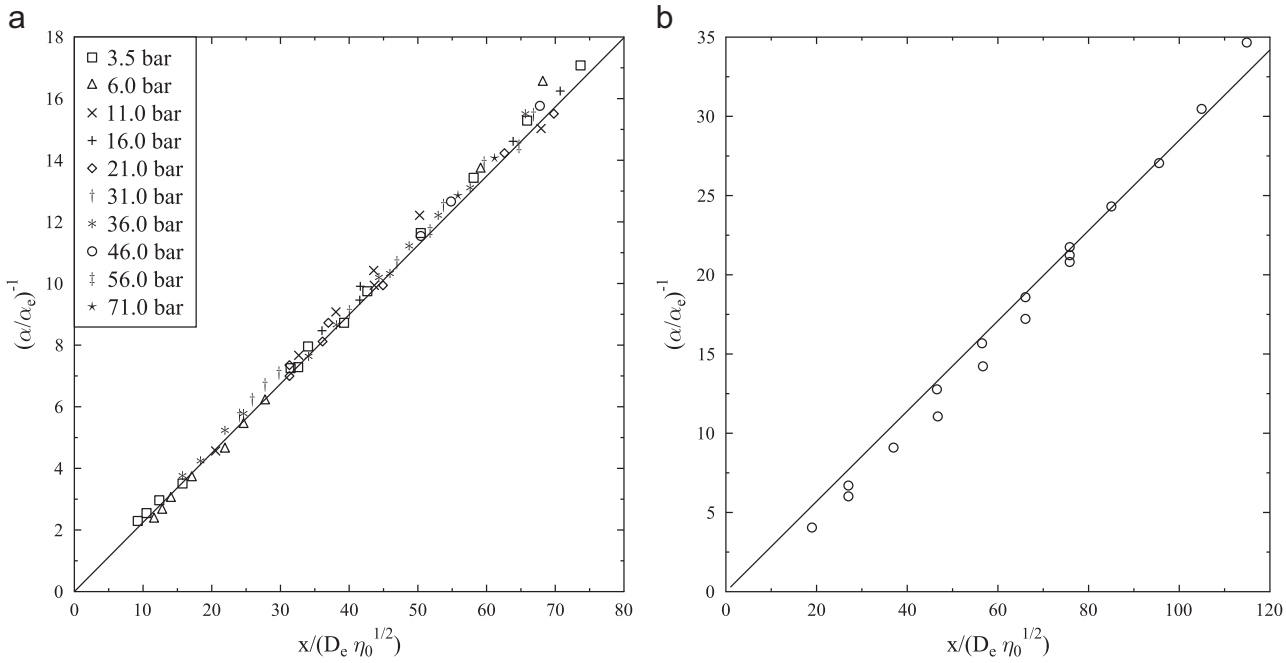

Fig. 17. Axial evolution of the volume fraction from [224]: (a) natural gas. and (b) ethylene ($\eta_0 = 8$).

Eventually, it is worth mentioning that each of the values given just now strongly depends on the experimental range used to obtain the correlation coefficient. This implies that a fair approach would be not only to mix all the measurements together (if feasible) but also to consider the influence of the range used for the fitting of the curve on the computed parameters.

At the present time, we thus propose to show how these methods have been used in order to model the decay of characteristic variables of the jet along the axis:

- In [224], we found some measurements of the volume fraction along the axis of natural gas and ethylene jets injected into air through a sonic nozzle operating on a pressure range $\eta_0 = 2-70$. However, the authors propose to use the effective diameter, computed with Eq. (25), instead of the exit diameter given by the relation (58) to model the axial evolution of the mass fraction. When compared with the experiments, shown in Fig. 17, a pretty good agreement is achieved. The decay constant κ is found to be independent of the fluid, its value being 4.90. Concerning the virtual origin a, different values are obtained (and additional data would be useful) yet they seem to be very small compared to the length.
- In [225], a similar approach is proposed to model the evolution of the axial velocity of air jets issued from a convergent nozzle on the same pressure range $\eta_0 = 2-75$. Yet, the proposed relation does not contain any density term, as the one in Eq. (58), and not only uses the effective diameter, as defined by Eq. (38), but also the equivalent velocity, computed by Eq. (37), as scaling parameters for the jet. The corresponding results are shown in Fig. 18. Here, the decay constant exhibits an increase with the pressure ratio, and a least square approximation leads to the value of 4.83. Meanwhile, an asymptotic value seems to be found at large pressures ($\eta_0 > 50$) for the virtual origin, even if a large scattering is observed, and consequent values are obtained. The associated measurements are given in Fig. 19. When using this approach for the volume fraction measurements of [224], a value of 5.4 is found for the decay constant, which is different from the previous result.
- In [57], one may find the only use of the model of [252] for underexpanded jets. Thus, the velocity along the centerline of air jets and one helium jet issuing from convergent nozzles are studied on the pressure range $\eta_0 = 5.7-20$. As we may see in Fig. 20, the measurements may be described this way if one uses the formulation of [253] for the decay constant ζ and modifies the abscissa to take into account the virtual origin and uses the equivalent diameter, calculated via Eq. (30), instead of the exit diameter. Finally, if the approximation for large abscissa is used, the comparison with the measurements of the mass fraction given by [224] leads to a value for the decay constant κ=4.6.
- In [244], a hydrogen tank pressurized at 100 bar is released through a nozzle and the volume fraction of H_2 is measured.

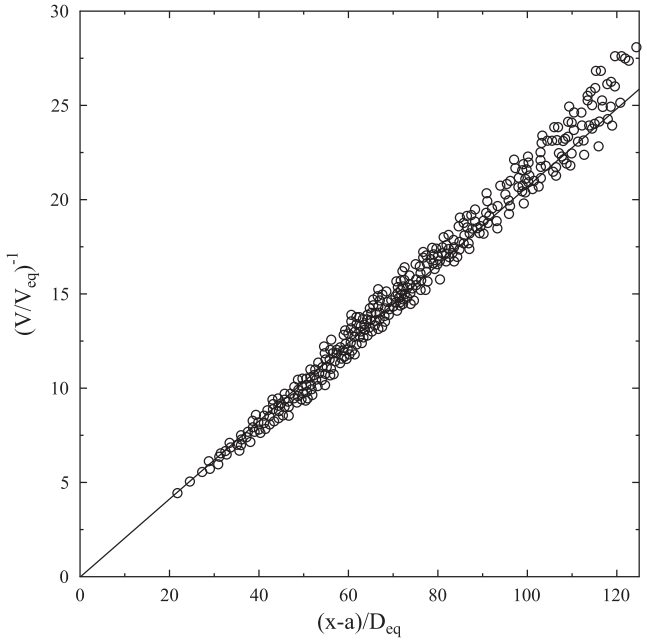

Fig. 18. Axial evolution of the velocity from [225].

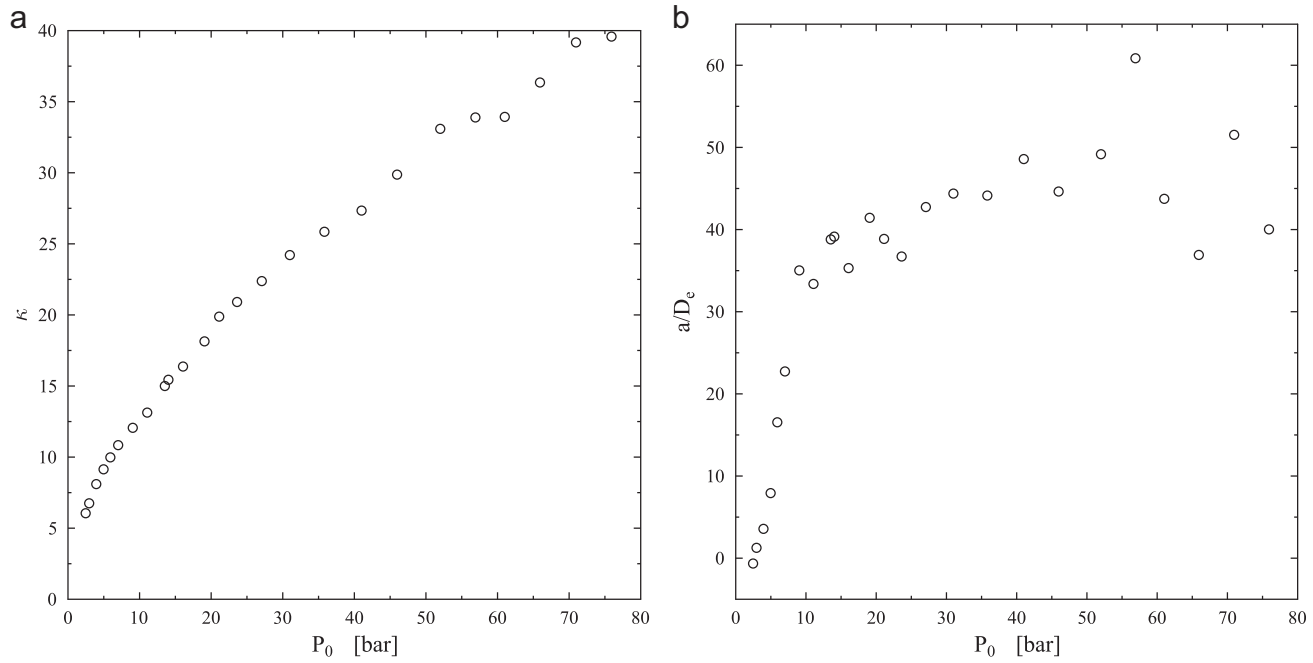

Fig. 19. Evolution of the parameters for the model for the velocity from [225]: (a) decay constant and (b) virtual origin.

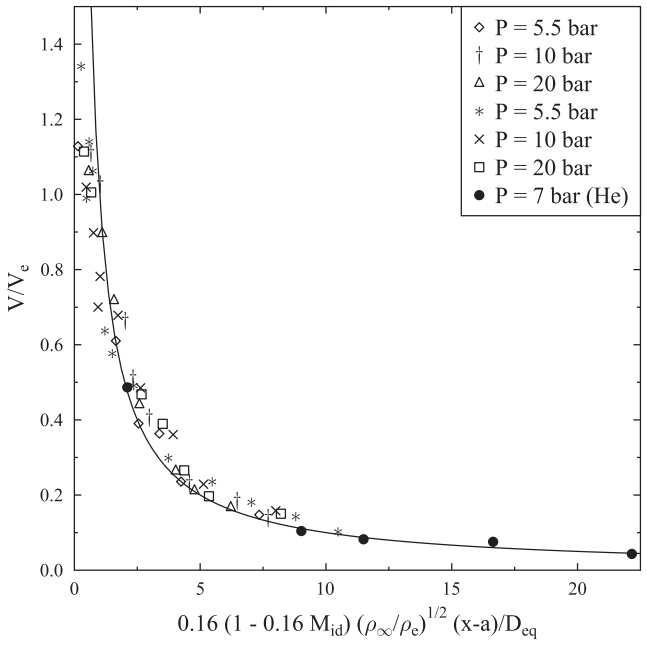

Fig. 20. Axial evolution of the velocity from [57].

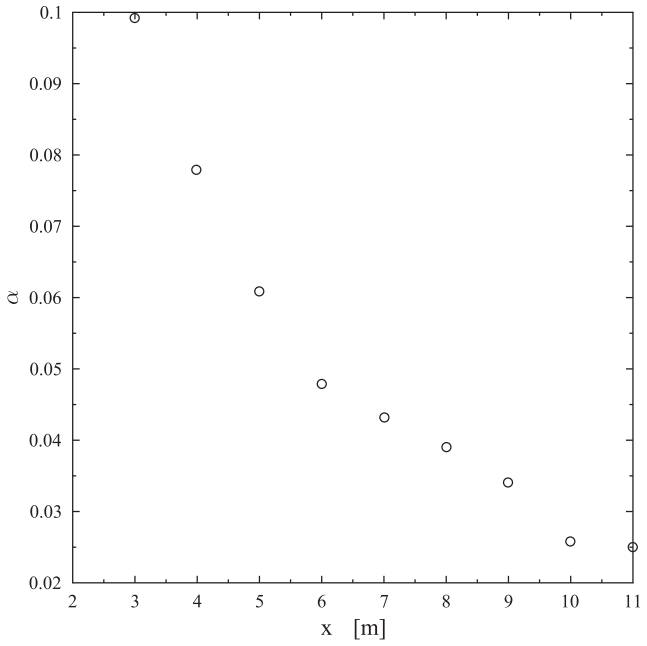

Fig. 21. Axial evolution of the mass fraction from [244].

The corresponding results are furnished in Fig. 21.

- In [251], a very pertinent analysis is done, in particular concerning the limits of some notional nozzle approaches and the difficulties inherent to the perfect gas hypothesis (especially when H_2 is concerned). Then, it is proposed to use Eq. (58) in its original form and, to do so, to compute the density of the jet using the underexpanded jet theory for an Abel-Noble equation of state, used for the dihydrogen. We present in Fig. 22 the comparison of this model with some measurements, unfortunately not available elsewhere.
- In [230], three nozzles are used to produce H_2 jets releasing in still air. The pressure range is one of the largest ever found for this kind of measurements, since it goes from 52 to 163. The corresponding results are given in Fig. 23. It is worth noticing here that the decay constant κ, for both the mass fraction and the velocity, is found to vary with the pressure ratio and a significant difference with the previous results is found (up to 34% for the mass fraction and to 160% for the velocity).
- In [231], the mass fractions of methane and hydrogen jets vented through orifices from a reservoir at 40 bar are reported. Using the pseudo-diameter approach of [224], a good agreement is obtained with the experiments as we may see in Fig. 24. Nevertheless, when normalizing by the densities ratio, the authors also found another value for the decay constant of $1/0.27 = 3.7$. Moreover, the virtual origin is indeed different from one fluid to another but it also cannot be neglected in the case of H_2 jet.
- In [247], the axial velocity of a H_2 jet issuing from a nozzle is

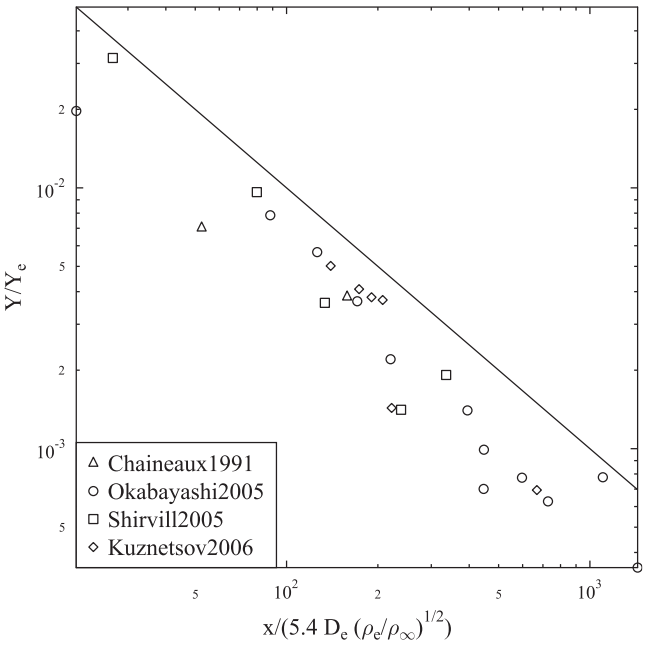

Fig. 22. Axial evolution of the mass fraction from [251].

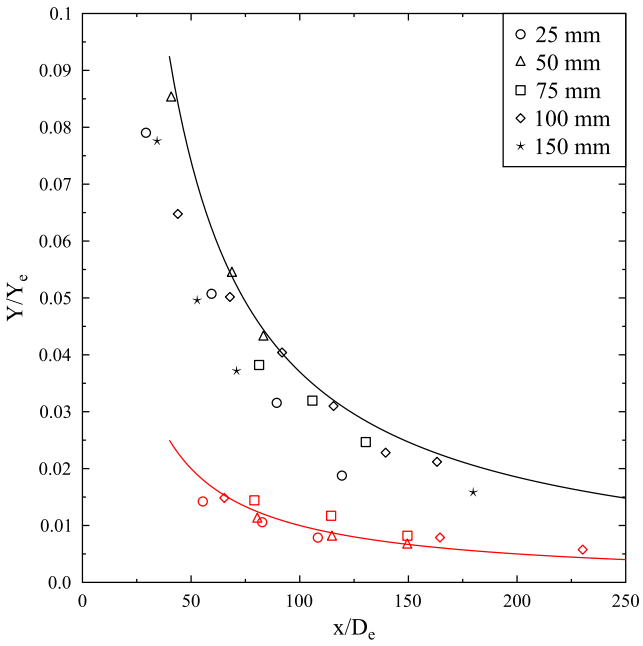

Fig. 24. Axial evolution of the mass fraction for a methane (black) and an hydrogen (red) jet from [231].

measured. Once more, the hyperbolic evolution well describes the flow behavior, as we may see in Fig. 25, yet the constant decay is found to be κ=5.1 and the exit diameter is used as in the original relation.

- In [248], hydrogen is still used and released from two orifices at pressure ratios ranging from 8.25 to 68.5. Here, it is still proposed to use the original relation to fit the measurements but using an adiabatic expansion approach to compute the equivalent density, using possibly a real gas equation of state. We present in Fig. 26 the evolution of the mass fraction and velocity.
- In [207], a convergent nozzle is used to release dried air at an exit pressure ratio $\eta_e = 1 - 20.3$. The adiabatic expansion approach (see upper) is then used to define scaling parameters. It then permits us to see that all experiments have a similar behavior, as shown in Fig. 27, when proper normalization is used. The universal decay constant is found to be $\kappa = 1/0.16 = 6.25$.

5.3. Conclusion

It is clear from all these experiments that the hyperbolic decay, predicted by incompressible theory, still holds in the case of under-expanded jets. Furthermore, it appears that the jet may be

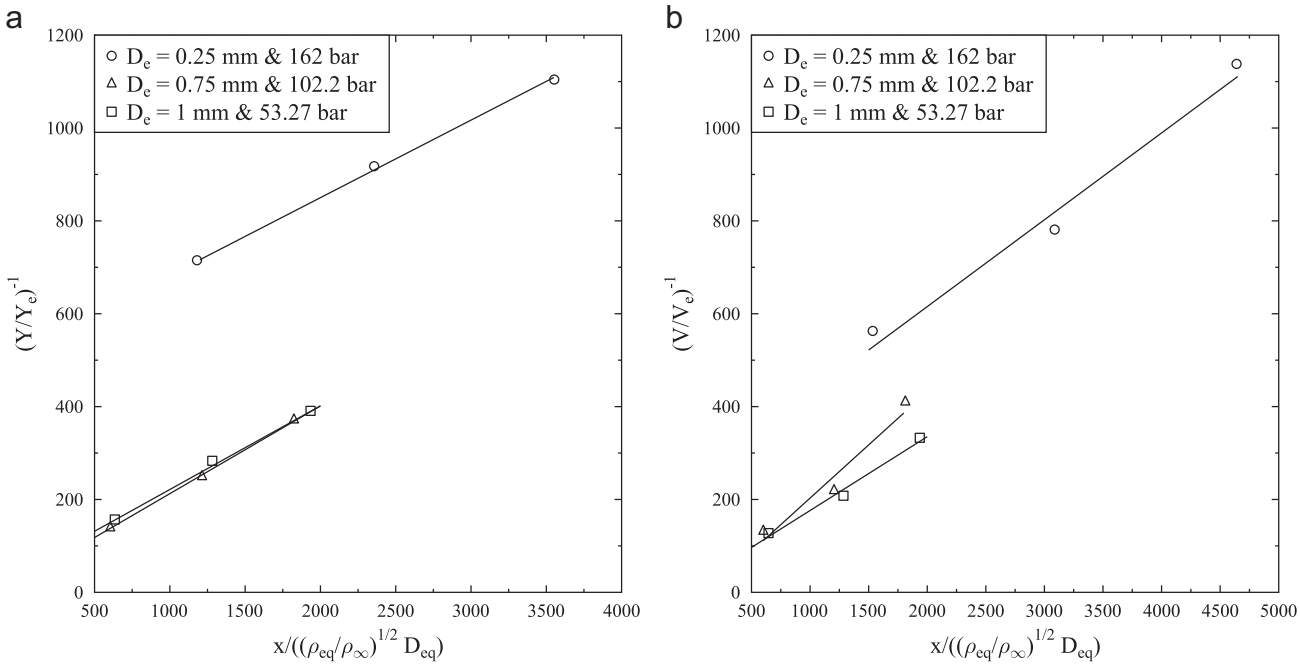

Fig. 23. Axial evolution from [230]: (a) mass fraction and (b) velocity. (For interpretation of the references to color in this figure caption, the reader is referred to the web version of this paper.)

approximated by an equivalent jet (notional nozzle approach) and the relations adapted to this effective jet. Nevertheless, we have seen that a great discrepancy exists between the results provided by the various modelings of this effective jet. Moreover, it seems that we may either use these artifacts or compute more precisely the state of the jet in this equivalent state (using in particular a correct thermodynamical modeling of the equation of state of the fluid) so as to reproduce the behavior of the variables. This implies that additional work is still needed to see what may be the best approach among these several ones. Thus, supplementary experiments at larger pressures would permit us to confirm (or not) if the decay constants, for the mass fraction and velocity, are really dependent on the pressure ratio and the associated correlation. By testing other fluids, we could also check if those constants are really universal, as they are supposed to be. Eventually, one could also consider under-expanded jets which are supersonic at the exit, since to our knowledge this has never been done.

6. Modeling approaches

We propose here to step through the principal available methods used to quantitatively describe the behavior of an underexpanded jet. Historically, the first approaches were based on theoretical considerations [95–97,29,67,33,136,72,141,137,99–101,208,140,42,127,103,43,204,105,210,46,47,13,107,211,246,108,255–261,129,178,179,53,165,180,181]. Generally, these studies used the method of characteristics, whose principle is to decompose the partial differential

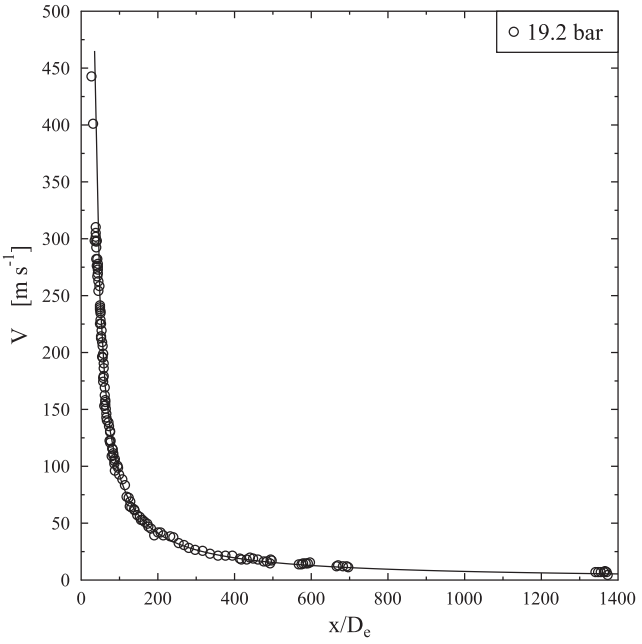

Fig. 25. Axial evolution of the velocity from [247].

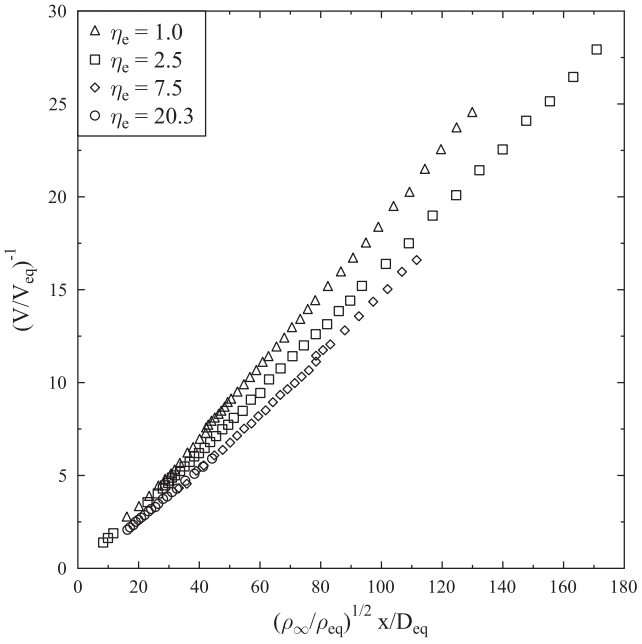

Fig. 27. Axial evolution of the velocity from [207].

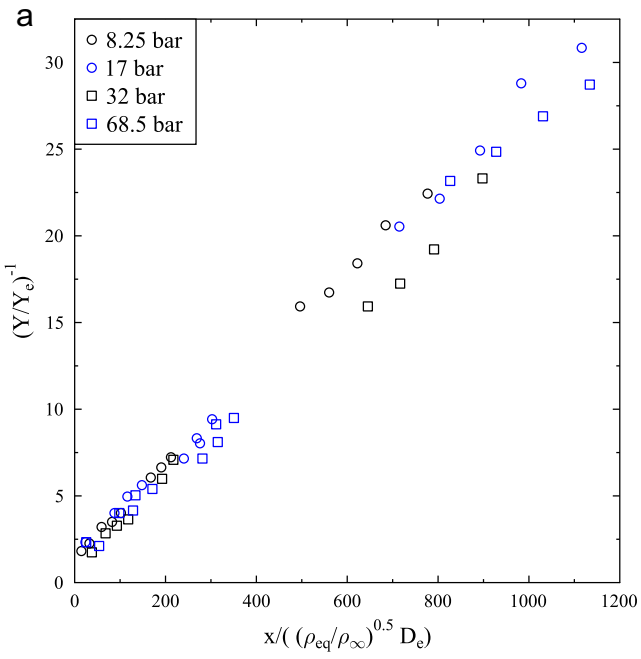

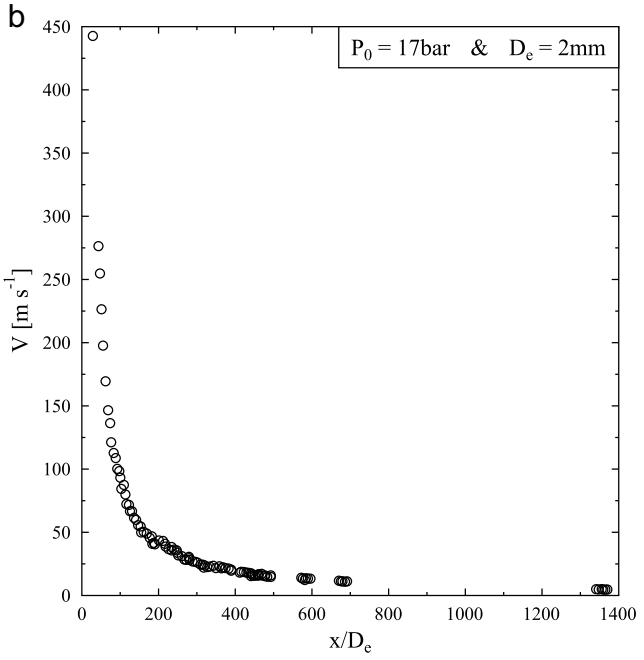

Fig. 26. Axial evolution from [248]: (a) mass fraction and (b) velocity.

equations describing the flow into ordinary differential equations which
are easily integrated along particular directions. Since the development of modern computers, and jointly of the numerical methods, it has become more and more useful to rely on numerical studies. These trends are now the main ones for three or four decades. The earlier works start to deal with simplified computations, such as the parabolized Navier–Stokes equations [27,148,175,112,37,215,222] or the thin-layer approximation [223]. Then, one may find some papers dealing with the Euler equations [138,111,147,75,36,214,17,81, 115,82,20,119,219,14,120,23,262–266,177]. Most often, they are based on finite difference schemes [147,36,214,115,82,14,264,265,177] even if now new ones used the finite volume method [138,75,81, 20,263,120,23] or even the finite element method [111]. It is seen that this kind of computations may give very accurate predictions of the variable in the core part of the flow, and a relatively good description of the shock wave pattern. Given the low computation cost associated with the inviscid hypothesis, it is clearly a boon if these features are the ones we are interested in. Should the study concern the behavior of the farfield zone or the mixing layer or any other feature of the flow where the viscous effects play a significant role, the modeling must now be based on the Navier–Stokes equations. Since the first numerical studies, and even now, the easiest way and the less expensive from a computational point of view is to consider the Reynolds Averaged Navier–Stokes equations (if obviously the flow is turbulent). Logically, this approach has been largely tested [110,31, 132,63,138,243,34,216,218,116,45,220,84,21,22,55,267–271,122,249], with the $k-\varepsilon$ model in an overwhelming majority of papers (be it its incompressible formulation or some of the proposed compressibility corrections of the $k-\varepsilon-CC$ class model). Even if this approach is acceptable to obtain the mean behavior of the flow, there are still some discrepancies between the results obtained with the various turbulence models ($k-\varepsilon$, $k-\varepsilon-$Realizable, $k-\varepsilon-RNG$, $k-\varepsilon-CC$, $k-\omega$, $k-\omega-SST$, $k-kl$, $k-R$, Reynolds Stress Model, etc.). More importantly, this forbids the study of any unsteadiness related phenomenon. In such a case, there is no other choice than considering the use of Large-Eddy Simulation or Direct Numerical Simulation. Currently the latter one is still unaffordable for entire simulation of underexpanded jets despite the huge progress in high performance computing, since the classical Reynolds number in such situations is of the order of 10^4-10^5 and the mesh length proportional to $\mathrm{Re}^{9/4}$ in any spatial direction. Actually, this also means that in the nearfield zone or at the initial stages of a release, DNS is the most powerful and reliable method. That is the spirit of the main studies dealing with such a method [191,212, 138,113,196,41,217,59,117,118,121,272,273,24,25]. Eventually, in all the other cases (that is to say in most cases), the LES seems to be the ideal compromise, be it ILES or classical LES methods using standard subgrid scale modelings. Surprisingly, as far as we know, there are not so much free jets simulations and the scarce ones mainly deal with moderately underexpanded jets [274–278,26]. This is particularly amazing since lots of these deal with such situations, and moreover we may find numerous studies dealing with impinging jets or jets in crossflows [279–282].

7. Thermodynamical behavior of the fluid

When one wants to model the release of a pressurized fluid, the equation of state has to be well chosen so as to correctly describe the behavior of the fluid. The main points this modeling must be able to predict unambiguously are the properties in the exit plane (pressure, temperature, density and velocity), the evolution of some characteristic parameters with the reducing pressure and temperature (sound velocity for example) and finally the potential

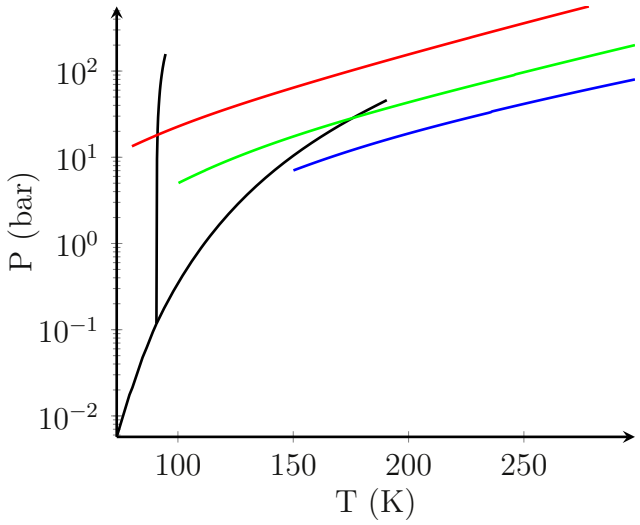

Fig. 28. Illustration of the possible appearance of a phase transition in a *P–T* diagram where various underexpanded jets conditions are considered.

appearance of another phase (liquid or solid).

Globally, the ideal gas equation of state is the most used. When dealing with air or relatively low pressure range, this does not raise any major problems and the use of an average polytropic coefficient may be sufficient enough. If not, a simple variation of γ with temperature or pressure may improve the results. However, it appears that the validity of the ideal gas does not hold with some species for high pressures, e.g. hydrogen or other supercritical fluid. Thus, the compressibility factor is far from unity and the real densities are very different from the ones computed with perfect gas equation of state and consequently the sound velocity is not well estimated [242,20,234,263,239,121,92].

Last but not least, it appears that the expansion of the fluid is inducing a high decrease in temperature and pressure which may drive the fluid into a metastable state [133,68,74,269,77,114,40, 203,283,238,121]. Logically, this may hypothetically allow the dynamic appearance of a phase, either liquid or even solid, as illustrated in Fig. 28. Depending on the initial conditions, the fluid undergoing the expansion may attain a final state which stays in the gas phase (blue path) or on the contrary lies in the liquid (green path) or solid phase (red path). In such a case, the apparition of this new phase will depend on the degree of supersaturation and on the time elapsed in this state, implying that this may also not happen even if feasible. Experimentally, condensation has been observed in underexpanded jets [157,267,74,15,284,130,123,65,205,184,92] and the appearance of a solid phase is well documented in the RESS (for Rapid Expansion of Supercritical Solution) process where a supercritical fluid is used as a solvent containing a solute which is seen to precipitate during the expansion. However, there is no overall study concerning the appearance of these new phases, as a function of the initial conditions or depending on the fluid involved in the jet, and so this point is still unclear. To highlight why these kind of studies may have some interest, from a practical point of view, it appears that the role of condensation in the properties of the Mach disk are ambiguous since [68] reported no noticeable effect while [74] noted a probable decrease of the Mach disk diameter and finally [285] noticed a strong influence on both the diameter and the location of the Mach disk. In the same way, injection of solid particles has shown to shorten the Mach disk location and to increase its curvature [83,259,86]. Since the Mach disk is composing the main part of the nearfield zone, which then serves as a starting point for reduced models in the farfield zone, one would appreciate to have a better description of this kind of phenomena.

Please cite this article as: E. Franquet, et al., Free underexpanded jets in a quiescent medium: A review, Progress in Aerospace Sciences (2015), http://dx.doi.org/10.1016/j.paerosci.2015.06.006

8. Conclusion

This paper has been devoted to the analysis of the experimental results available for axisymmetric free underexpanded jets ejected in a fluid at rest. It appears that even if the global structure of such jets is perfectly known nowadays, there are still many features either ill-known or completely ignored. These shortcomings arise from the uncertainties of the available measurements on one hand, and from a lack of studies on the other hand. Along with this study, the various numerical methods and the associated thermodynamical issues have been briefly discussed, emphasizing on the global strengths and weaknesses of both.

To summarize the main conclusions drawn in the present paper, it has been shown that, for the nearfield zone, the position of the Mach disk is pretty well described. However there remains some doubt concerning its diameter and the exact conditions leading to its appearance. Furthermore, there is clearly a lack of information when one seeks for a quantitative expression of the diameter of the jet and of the wave-length of the cells structure and of the total length of the potential core. When dealing with the farfield zone, one may be pretty confident about the hyperbolic decay for all the variables, similar to the incompressible case. Moreover, the notional nozzle is clearly a well-suited approach to represent the behavior of such jets. Nonetheless, there is still some work to do in order to discriminate the best model among the several ones available and also to determine first if the decay constants are really universal and second their corresponding values. Furthermore, all these studies have been developed only for sonic jets at the exit, and so the influence of the Mach number is not visible. Finally, we would like to point out the various phenomenon which are badly managed: the curvature of the Mach disk and disappearance of the cells when the pressure ratio increases, the characteristic lengths of the jets, the importance and beginning of the entrainment of the external fluid, the viscous effects in the mixing layer (transition to turbulence, interactions with the hydrodynamic instabilities, etc.). To our opinion, the two last points may be of importance for the pollution and the dilution of hot gases of combustible species.

Eventually, once the above features could be better known, it would be interesting to consider the influence of the ambient fluid, particularly when it is also moving, i.e. to perform the same analysis for underexpanded jets in a co- or cross-flow. On the other hand, although the results are qualitatively the same for non-symmetric jets, a quantitative review of associated results remains undone.

Appendix A. Isentropic relations for a perfect gas

A.1. Expressions in function of the Mach number and the stagnation state

$$\frac{P_0}{P} = \left(1 + \frac{\gamma - 1}{2} M^2\right)^{\gamma/(\gamma-1)} \tag{60}$$

$$\frac{T_0}{T} = 1 + \frac{\gamma - 1}{2} M^2 \tag{61}$$

$$\frac{\rho_0}{\rho} = \left(1 + \frac{\gamma - 1}{2} M^2\right)^{1/(\gamma-1)} \tag{62}$$

Remark: for an underexpanded jet, the ideally expanded state is defined as the one where the pressure in the flow would be the same as the ambient one. Using Eq. (60), it implies that the ideally expanded Mach number is

$$M_{id} = \sqrt{\frac{2}{\gamma - 1}\left(\eta_0^{(\gamma-1)/\gamma} - 1\right)} \tag{63}$$

A.2. Expressions in function of the Mach number and the critical state

$$\frac{P^\star}{P} = \left(\frac{1 + \frac{\gamma - 1}{2} M^2}{\frac{\gamma + 1}{2}}\right)^{\gamma/(\gamma-1)} \tag{64}$$

$$\frac{T^\star}{T} = \frac{1 + \frac{\gamma - 1}{2} M^2}{\frac{\gamma + 1}{2}} \tag{65}$$

$$\frac{\rho^\star}{\rho} = \left(\frac{1 + \frac{\gamma - 1}{2} M^2}{\frac{\gamma + 1}{2}}\right)^{1/(\gamma-1)} \tag{66}$$

$$\frac{A}{A^\star} = \frac{1}{M}\left(\frac{1 + \frac{\gamma - 1}{2} M^2}{\frac{\gamma + 1}{2}}\right)^{(1/2)(\gamma+1)/(\gamma-1)} \tag{67}$$

A.3. Relations between stagnation and critical state

$$\frac{P^\star}{P_0} = \left(\frac{2}{\gamma + 1}\right)^{\gamma/(\gamma-1)} \tag{68}$$

$$\frac{T^\star}{T_0} = \frac{2}{\gamma + 1} \tag{69}$$

$$\frac{\rho^\star}{\rho_0} = \left(\frac{2}{\gamma + 1}\right)^{1/(\gamma-1)} \tag{70}$$

Appendix B. Normal shock relations for a perfect gas

B.1. Expressions in function of the Mach number before and after the shock

$$\frac{P_1 M_1}{\sqrt{T_1}} = \frac{P_2 M_2}{\sqrt{T_2}} \tag{71}$$

$$\frac{P_2}{P_1} = \frac{1 + \gamma M_1^2}{1 + \gamma M_2^2} \tag{72}$$

$$\frac{T_2}{T_1} = \frac{1 + \frac{\gamma - 1}{2} M_1^2}{1 + \frac{\gamma - 1}{2} M_2^2} \tag{73}$$

B.2. Expressions in function of the Mach number before the shock

$$\frac{P_2}{P_1} = \frac{2\gamma}{\gamma + 1} M_1^2 - \frac{\gamma - 1}{\gamma + 1} = \frac{2\gamma}{\gamma + 1}\left(M_1^2 - 1\right) + 1 \tag{74}$$

Please cite this article as: E. Franquet, et al., Free underexpanded jets in a quiescent medium: A review, Progress in Aerospace Sciences (2015), http://dx.doi.org/10.1016/j.paerosci.2015.06.006

$$\frac{T_2}{T_1} = \frac{2(\gamma-1)}{(\gamma+1)^2}\frac{\left(1+\frac{\gamma-1}{2}M_1^2\right)\left(\frac{2\gamma}{\gamma-1}M_1^2-1\right)}{M_1^2} \tag{75}$$

$$\frac{\rho_2}{\rho_1} = \frac{\gamma+1}{2}\frac{M_1^2}{1+\frac{\gamma-1}{2}M_1^2} \tag{76}$$

Appendix C. Discharge coefficient

We have seen that some authors choose to introduce the discharge coefficient in order to take into account what is known as the *vena contracta* effect. Inasmuch as this phenomenon may modify the exit conditions, compared to the isentropic ones, it may be worth considering it, be it for the study of the nearfield zone (particularly the position and diameter of the Mach disk) or for the farfield zone (since the equivalent jet is determined from the exit conditions). Yet, we will not detail here how to compute this coefficient since it is a huge task which is largely studied in the literature. Instead, we will just recall the main reasons for such a behavior and their consequences in order to highlight the situations where it may be useful to insert such a detail in the computations. The interested reader is referred to the 9300 ISO Standard or to the Euromet works, and associated papers, if supplementary information is required or to the discussions available in [62,56,224,286,287,81,117,14,53,261,170,172] in the case of underexpanded jets.

To briefly recall the major points, the discharge coefficient is introduced so as to better describe the real mass flow of any device, since this one may vary from the ideally isentropic one. Thus it is defined as follows:

$$C_D = \frac{\dot{m}_{\text{real}}}{\dot{m}_{\text{isent.}}} \tag{77}$$

In the case of perfect gas, the ideal mass flow rate at choked conditions is easy to compute and consequently we may write

$$\frac{\dot{m}_{\text{real}}}{A} = C_D\, C^\star \frac{P_0}{\sqrt{RT_0}} \tag{78}$$

with $C^\star = \sqrt{\gamma\left(\frac{2}{\gamma+1}\right)^{(\gamma+1)/(\gamma-1)}}$.

As we may see, the discharge coefficient C_D thus permits us to take into account the various effects that may modify the mass flow rate. Among these ones, one may cite

- the curvature of the streamlines (in particular with convergent nozzles or orifices) since they are often still converging when attaining the exit and therefore they become parallel only downstream of the exit.
- the viscous effects, especially the apparition of a transition in the boundary layer.
- the real gas effects, in particular at extreme pressure or temperature where the fluid may have a behavior far from that of an ideal gas.

Appendix D. Overview of the various studies dealing with the structure of underexpanded jets

See Tables 2–4.

References

[1] A.J.C. de Saint-Venant, P.L. Wantzel, Mémoire et expériences sur l'écoulement de l'air, J. Ecole Polytech. (Paris) 16 (1839) 85–122.
[2] P. Salcher, J. Whitelaw, Uber den ausfluss stark verdichteter luft, Sitz. Akad. Wiss. Wien 98 (1889) 267–287.
[3] E. Mach, P. Salcher, Photographische Fixierung der durch Projectile in der Luft eingeleiteten Vorgänge, Sitz. Akad. Wiss. Wien 2 (1887) 764–787.
[4] E. Mach, P. Salcher, Optische Untersuchungen der Luftstrahlen, Sitz. Akad. Wiss. Wien 98 (1889) 1303–1309.
[5] R. Emden, Flow phenomena in permanent gases, Ann. D Phys. U Chem. 69 (1899) 426.
[6] L. Prandtl, Uber die stationären wellen in einem gasstrahl, Phys. Z. 5 (1904) 599–601.
[7] L. Prandtl, Beiträge zur theorie der dampfströmung durch düsen, VDI-Z 48 (1904) 348–350.
[8] L. Prandtl, Neue untersuchungen über die strömende bewegung der gase und dämpfe, Phys. Z. 8 (1907) 23–30.
[9] R. Courant, K.O. Friedrichs, Supersonic Flow and Shock Waves, Interscience, Springer, New York, 1956.
[10] A. Shapiro, The Dynamics and Thermodynamics of Compressible Fluid Flow, vol. 1, The Ronald Press Company, New York, 1953.
[11] R.D. Zucker, O. Biblarz, Fundamentals of Gas Dynamics, second edition,. John Wiley & Sons, Ltd, Hoboken, New Jersey, 2002.
[12] R.T. Driftmyer, A correlation of freejet data, AIAA J. 10 (1972) 1093–1095.
[13] J.L. Palmer, R.K. Hanson, Application of method of characteristics to underexpanded, freejet flows with vibrational nonequilibrium, AIAA J. 36 (2) (1998) 193–200.
[14] Y. Otobe, H. Kashimura, S. Matsuo, T. Setoguchi, H.-D. Kim, Influence of nozzle geometry on the near-field structure of a highly underexpanded sonic jet, J. Fluids Struct. 24 (2) (2008) 281–293.
[15] A.V. Eremin, V.A. Kochnev, A.A. Kulikovskii, I.M. Naboko, Nonstationary processes in starting strongly underexpanded jets, J. Appl. Mech. Tech. Phys. 19 (1978) 27–31.
[16] V.V. Golub, Development of shock wave and vortex structures in unsteady jets, Shock Waves 3 (4) (1994) 279–285.
[17] V.V. Golub, D.I. Baklanov, T.V. Bazhenova, M.V. Bragin, S.V. Golovastov, M.F. Ivanov, V.V. Volodin, Shock-induced ignition of hydrogen gas during accidental or technical opening of high-pressure tanks, J. Loss Prev. Process Ind. 20 (4–6) (2007) 439–446.
[18] R. Ishii, H. Fujimoto, N. Hatta, Y. Umeda, Experimental and numerical analysis of circular pulse jets, J. Fluid Mech. 392 (1999) 129–153.
[19] N.G. Korobeishchikov, A.E. Zarvin, V.Zh. Madirbaev, Hydrodynamics of pulsed supersonic underexpanded jets: spatiotemporal characteristics, Tech. Phys. 49 (8) (2004) 973–981.
[20] R. Khaksarfard, M.R. Kameshi, M. Paraschivoiu, Numerical simulation of high pressure release and dispersion of hydrogen into air with real gas model, Shock Waves 20 (2010) 205–216.
[21] Yumiko Otobe, Tsuyoshi Yasunobu, Hideo Kashimura, Shigeru Matsuo, Toshiaki Setoguchi, Heuy Dong Kim, Hysteretic phenomenon of underexpanded moist air jet, AIAA J. 47 (12) (2009) 2792–2799.
[22] F. Péneau, G. Pedro, P. Oshkai, P. Bénard, N. Djilali, Transient supersonic release of hydrogen from a high pressure vessel: a computational analysis, Int. J. Hydrog. Energy 34 (14) (2009) 5817–5827 (2nd International Conference on Hydrogen Safety).
[23] M.I. Radulescu, C.K. Law, The transient start of supersonic jets, J. Fluid Mech. 578 (2007) 331–369.
[24] B.P. Xu, L. el Hima, J.X. Wen, S. Dembele, V.H.Y. Tam, T. Donchev, Numerical study on the spontaneous ignition of pressurized hydrogen release through a tube into air, J. Loss Prev. Process Ind. 21 (2) (2008) 205–213 (Hydrogen Safety).
[25] B.P. Xu, L. EL Hima, J.X. Wen, V.H.Y. Tam, Numerical study of spontaneous ignition of pressurized hydrogen release into air, Int. J. Hydrog. Energy 34 (14) (2009) 5954–5960.
[26] B.P. Xu, J.X. Wen, S. Dembele, V.H.Y. Tam, S.J. Hawksworth, The effect of pressure boundary rupture rate on spontaneous ignition of pressurized hydrogen release, J. Loss Prev. Process Ind. 22 (3) (2009) 279–287.
[27] K. Abdol-Hamid, R. Wilmoth, Multiscale turbulence effects in underexpanded supersonic jets, AIAA J. 27 (1989) 315–322.
[28] G.N. Abramovich, The Theory of Turbulent Jets, MIT Press, Cambridge, Mass, 1963.
[29] T.C. Adamson, J.A. Nicholls, On the structure of jets from highly underexpanded nozzles into still air, J. Aerosp. Sci. 26 (1959) 16–24.
[30] A.V. Antsupov, General properties of underexpanded and overexpanded supersonic gas jets, Sov. Phys. Tech. Phys. 19 (2) (1974) 234–238.
[31] Y. Avital, G. Cohen, L. Gamss, Y. Kanelbaum, J. Macales, B. Trieman, S. Yaniv, M. Lev, J. Stricker, A. Sternlieb, Experimental and computational study of infrared emission from underexpanded rocket exhaust plumes, J. Thermophys. Heat Transf. 15 (1) (2001) 377–383.
[32] L.H. Back, R.B. Cuffel, Viscous slipstream flow downstream of a centerline Mach reflection, AIAA J. 9 (1971) 2107–2109.
[33] A.B. Bauer, Normal shock location of underexpanded gas-particle jets, AIAA J. 3 (6) (1965) 1187–1189.
[34] P.S. Cumber, M. Fairweather, S.A.E.G. Falle, J.R. Giddings, Predictions of the structure of turbulent, highly underexpanded jets, J. Fluids Eng. 117 (4) (1995) 599–604.
[35] N.J. Dam, M. Rodenburg, R.A.L. Tolboom, G.G.M. Stoffels, P.M. Huisman Kleinherenbrink, J.J. Ter Meulen, Imaging of an underexpanded nozzle flow by UV laser Rayleigh scattering, Exp. Fluids 24 (2) (1998) 93–101.
[36] S.M. Dash, P.D. Del Guidice, Analysis of three-dimensional ducted and exhaust plume flowfields, AIAA J. 16 (1979) 823–830.
[37] S.M. Dash, D.E. Wolf, Interactive phenomena in supersonic jet mixing problems. Part I: phenomenology and numerical modeling techniques, AIAA J. 22 (7) (1984) 905–913.
[38] C.D. Donaldson, R.S. Snedeker, A study of free jet impingement. Part 1. Mean properties of free and impinging jets, J. Fluid Mech. 45 (2) (1971) 281–319.

Please cite this article as: E. Franquet, et al., Free underexpanded jets in a quiescent medium: A review, Progress in Aerospace Sciences (2015), http://dx.doi.org/10.1016/j.paerosci.2015.06.006

[39] P.L. Eggins, D.A. Jackson, Laser-doppler velocity measurements in an under-expanded free jet, J. Phys. D: Appl. Phys. 7 (14) (1974) 1894.
[40] I.A. Graur, T.G. Elizarova, A. Ramos, G. Tejeda, J.M. Fernández, S. Montero, A study of shock waves in expanding flows on the basis of spectroscopic experiments and quasi-gasdynamic equations, J. Fluid Mech. 504 (2004) 239–270.
[41] B.J. Gribben, K.J. Badcock, B.E. Richards, Numerical study of shock-reflection hysteresis in an underexpanded jet, AIAA J. 38 (2) (2000) 275–283.
[42] R. Ladenburg, C.C. Van Voorhis, J. Winckler, Interferometric studies of faster than sound phenomena. Part II. Analysis of supersonic air jets, Phys. Rev. 76 (1949) 662–677.
[43] E.S. Love, C.E. Grigsby, L.P. Lee, J.M. Woodling, Experimental and theoretical studies of axisymmetric free jets, Technical Report R-6, NASA, 1959.
[44] N. Menon, B.W. Skews, Rectangular underexpanded gas jets: effect of pressure ratio, aspect ratio and mach number, in: Klaus Hannemann, Friedrich Seiler (Eds.), Shock Waves, Springer, Berlin, Heidelberg, 2009, pp. 991–996.
[45] N. Menon, B.W. Skews, Shock wave configurations and flow structures in non-axisymmetric underexpanded sonic jets, Shock Waves 20 (3) (2010) 175–190.
[46] D.C. Pack, On the formation of shock-waves in supersonic gas jets, Q. J. Mech. Appl. Math. 1 (1) (1948) 1–17.
[47] D.C. Pack, A note on Prandtl's formula for the wavelength of a supersonic gas jet, Q. J. Mech. Appl. Math. 3 (2) (1950) 173–181.
[48] E. Rajakuperan, M.A. Ramaswamy, An experimental investigation of under-expanded jets from oval sonic nozzles, Exp. Fluids 24 (4) (1998) 291–299.
[49] M. Rasi, R. Saintola, K. Valli, Visualizing the expanding flow of gas from helium-jet and ion-guide nozzles, Nucl. Instrum. Methods Phys. Res. Sect. A: Accel. Spectrom. Detect. Assoc. Equip. 378 (1–2) (1996) 251–257.
[50] J. Reid, R.C. Hastings, The effect of central jet on the base pressure of a cylindrical after-body in a supersonic stream, Technical Report, Ministry of Aviation, 1959.
[51] J.M. Seiner, T.D. Norum, Experiments of shock associated noise of supersonic jets, AIAA Paper, 1979, p. 1526.
[52] J.M. Seiner, T.D. Norum, Aerodynamic aspects of shock containing jet plumes, AIAA Paper, 1980, p. 0965.
[53] A.R. Vick, E.H. Andrews, J.S. Dennard, C.B. Craidon, Comparisons of experimental free-jet boundaries with theoretical results obtained with the method of characteristics, Technical Note D-2327, NASA, 1964.
[54] J.A. Wilkes, P.M. Danehy, R.J. Nowak, D.W. Alberfert, Fluorescence imaging study of impinging underexpanded jets, in: 46th AIAA Aerospace Sciences Meeting and Exhibit, 2008.
[55] A.J. Saddington, N.J. Lawson, K. Knowles, An experimental and numerical investigation of under-expanded turbulent jets, Aeronaut. J. 108 (1081) (2004) 145–152.
[56] A.P. Aleshin, I.N. Denisov, N.M. Rogachev, V.F. Sivirkin, Effect of the cone angle and the degree of contraction of a sonic nozzle on the geometrical structure of the first roll of an underexpanded jet, J. Eng. Phys. Thermophys. 28 (1975) 207–210.
[57] B.C.R. Ewan, K. Moodie, Structure and velocity measurements in underexpanded jets, Combust. Sci. Technol. 45 (5–6) (1986) 275–288.
[58] Andrea G. Hsu, Ravi Srinivasan, Rodney D. Bowersox, Simon W. North, Molecular tagging using vibrationally excited nitric oxide in an underexpanded jet flowfield, AIAA J. 47 (11) (2009).
[59] T. Matsuda, Y. Umeda, R. Ishii, A. Yasuda, K. Sawada, Numerical and experimental studies on choked underexpanded jets, vol. 49, Memoirs of the Faculty of Engineering, Kyoto University, 1987, pp. 84–110.
[60] L.N. Ung, G.K. Hargrave, An investigation of underexpanded free jets from straight nozzles, in: 1st International Conference on Optical and Laser Diagnostics, vol. 177, 2003, pp. 39–44.
[61] J.A. Wilkes, P.M. Danehy, R.J. Nowak, Fluorescence imaging study of transition in underexpanded jets, in: 21st International Congress on Instrumentation in Aerospace Simulation Facilities, 2005, iciasf '05, 2005, pp. 1–8.
[62] A.L. Addy, Effects of axisymmetric sonic nozzle geometry on Mach disk characteristics, AIAA J. 19 (1) (1981) 121–122.
[63] P. Birkby, G.J. Page, Numerical predictions of turbulent underexpanded sonic jets using a pressure-based methodology, Proc. Inst. Mech. Eng. Part G: J. Aerosp. Eng. 215 (3) (2001) 165–173.
[64] J.C. Gibbings, J. Ingham, D. Johnson, Flow in a supersonic jet expanding from a convergent nozzle, Technical Report, Aeronautical Research Council, 1972.
[65] A. Krothapalli, G. Buzyna, L. Lourenco, Streamwise vortices in an underexpanded axisymmetric jet, Phys. Fluids A 3 (8) (1991) 1848–1851.
[66] B. André, T. Castelain, C. Bailly, Experimental exploration of underexpanded supersonic jets, Shock Waves 24 (2014) 21–32.
[67] H. Ashkenas, F.S. Sherman, The structure and utilization of supersonic free jets in low density wind tunnels, in: Proceedings of the 4th International Symposium on Rarefied Gas Dynamics, vol. 2(7), 1964, pp. 84–105.
[68] V.S. Avduevskii, A.V. Ivanov, I.M. Karpman, V.D. Traskovskii, M.Ya. Yudelovich, Flow in supersonic viscous underexpanded jet, Fluid Dyn. 5 (1970) 409–414.
[69] V.S. Avduevskii, A.V. Ivanov, I.M. Karpman, V.D. Traskovskii, M.Ya. Yudelovich, Effect of viscosity on the flow in the initial part of a highly underexpanded jets, Sov. Phys. Dokl. Fluid Mech. 16 (3) (1971) 186–189.
[70] V.S. Avduevskii, A.V. Ivanov, I.M. Karpman, V.D. Traskovskii, M.Ya. Yudelovich, Structure of turbulent underexpanded jets issuing into an immersed space and coflow, Fluid Dyn. 7 (3) (1972) 380–391.
[71] K. Bier, B. Schmidt, Form of compression shocks in freely expanding gas jets, Zeit. Angew. Phys. 13 (1961) 493–500.
[72] F.S. Billig, R.C. Orth, M. Lasky, Unified analysis of gaseous jet penetration, AIAA J. 9 (6) (1971).
[73] F.I. Buckley Jr, Mach disk location in jets in co-flowing airstreams, AIAA J. 13 (1975) 105–106.
[74] S. Crist, P.M. Sherman, D.R. Glass, Study of the highly underexpanded sonic jet, AIAA J. 4 (1966) 68–71.
[75] D. D'Ambrosio, L.M. De Socio, G. Gaffuri, Physical and numerical experiments on an under-expanded jet, Meccanica 34 (1999) 267–280, http://dx.doi.org/10.1023/A:1004799204306.
[76] L. D'Attore, F. Harshbarger, Further experimental and theoretical studies of underexpanded jets near the Mach disc, Technical Report, Defense Documentation Center, 1964.
[77] M.D. Di Rosa, A.Y. Chang, R.K. Hanson, Continuous wave dye-laser technique for simultaneous, spatially resolved measurements of temperature, pressure, and velocity of NO in an underexpanded free jet, Appl. Opt. 32 (21) (1993) 4074–4087.
[78] Yu.P. Finat'ev, L.A. Shcherbakov, N.M. Gorskaya, Mach number distribution over the axis of supersonic underexpanded jets, J. Eng. Phys. 15 (1968) 1153–1157.
[79] G.I. Gannochenko, L.S. Ermolayev, N.A. Zadorozhnyi, On the position of the central compression shock in an underexpanded sonic jet issuing from a slot nozzle, J. Appl. Mech. Tech. Phys. 4 (1986) (89+91).
[80] Yu.A. Gostintsev, V.V. Zelentsov, V.S. Ilyukhin, P.F. Pokhil, Structure of under-expanded supersonic swirling gas jet, Fluid Dyn. 4 (5) (1969) 105–107.
[81] K. Hatanaka, T. Saito, Influence of nozzle geometry on underexpanded axisymmetric free jet characteristics, Shock Waves 22 (2012) 427–434.
[82] H. Katanoda, Y. Miyazato, M. Masuda, K. Matsuo, Pitot pressures of correctly-expanded and underexpanded free jets from axisymmetric supersonic nozzles, Shock Waves 10 (2) (2000) 95–101.
[83] C.H. Lewis Jr, D.J. Carlson, Normal shock location in underexpanded gas and gas-particle jets, AIAA J. 2 (4) (1964) 776–777.
[84] Y. Otobe, S. Matsuo, M. Tanaka, H. Kashimura, T. Setoguchi, A study on characteristics of under-expanded condensing jet, JSME Int. J. Ser. B Fluids Therm. Eng. 49 (4) (2006) 1165–1172.
[85] W.J. Sheeran, D.S. Dosanjh, Observations on jet flows from a two-dimensional, underexpanded, sonic nozzle, AIAA J. 6 (1968) 540–542.
[86] M. Sommerfeld, The structure of particle-laden, underexpanded free jets, Shock Waves 3 (1994) 299–311.
[87] Katsu'ine Tabei, Hiroyuki Shirai, Fumio Takakusagi, Density measurements of underexpanded free jets of air from circular and square nozzles by means of Moiré–Schlieren method, JSME Int. J. 35 (2) (1992) 212–217.
[88] V.V. Volchkov, A.V. Ivanov, Thickness and internal structure of a normal shock formed by discharge of a highly underexpanded jet into a low-density space, Fluid Dyn. 4 (1969) 113–115, http://dx.doi.org/10.1007/BF01025156.
[89] M.J. Werle, D.G. Shaffer, R.T. Driftmyer, On freejet terminal shocks, AIAA J. 8 (1970) 2295–2297.
[90] Donald E. Wilcox, Alexander Weir Jr, J.A. Nicholls, Roger Dunlap, Location of Mach discs and diamonds in supersonic air jets, J. Aeronaut. Sci. 24 (2) (1957) 145–160.
[91] J.A. Wilkes, C.E. Glass, P.M. Danehy, R.J. Nowak, Fluorescence imaging of under-expanded jets and comparison with CFD, Technical Report, NASA, 2007, AIAA.
[92] P.-K. Wu, T.H. Chen, Injection of supercritical ethylene in nitrogen, J. Propuls. Power 12 (4) (1996) 770–777.
[93] B. Yip, K. Lyons, M. Long, Visualization of a supersonic underexpanded jet by planar Rayleigh scattering, Phys. Fluids A 1 (9) (1989) 1449–1450.
[94] V.I. Zapryagaev, V.I. Kornilov, A.V. Lokotko, Experimental investigation of shock wave structure and streamwise vortices in supersonic jet, in: 4th European Symposium on Aerothermodynamics for Space Applications, 2002.
[95] A.N. Abdelhamid, D.S. Dosanjh, Mach disk and Riemann wave in underexpanded jet flows, AIAA J. 6 (1969) 69–665.
[96] M. Abbett, Mach disk in underexpanded exhaust plumes, AIAA J. 9 (3) (1971) 512–514.
[97] F. Albini, Approximate computation of underexpanded jet structure, AIAA J. 3 (8) (1965) 1535–1537.
[98] J. Bowyer, L. D'Attore, H. Yoshihara, Transonic aspects of hypervelocity rocket plumes, in Supersonic Flow, Chemical Processes and Radiative Transfer, Pergamon Press, London, 1964, pp. 201–210.
[99] I.S. Chang, W.L. Chow, Mach disc from underexpanded axisymmetric nozzle flow, AIAA J. 12 (8) (1974) 1079–1082.
[100] D.W. Eastman, L.P. Radtke, Location of the normal shock wave in the exhaust plume of a jet, AIAA J. 1 (1963) 918–919.
[101] J.H. Fox, On the structure of jet plumes, AIAA J. 12 (1974) 105–107.
[102] C.N. Kelber, S. Jarvis Jr, An analysis of the gas flow from a very high pressure nozzle. Technical Report, Frankford Arsenal, 1952.
[103] J.C. Lengrand, J. Allègre, M. Raffin, Underexpanded free jets and their interaction with adjacent surfaces, AIAA J. 14 (1982) 4011.
[104] J.P. Moran, Similarity in high-altitude jets, AIAA J. 5 (7) (1967) 1343–1345.
[105] I.N. Murzinov, Similarity parameters for the escape of a strongly underexpanded jet into a flooded space, Fluid Dyn. 6 (1971) 675–680.
[106] C.E. Peters, W.J. Phares, The structure of plumes from moderately underexpanded supersonic nozzle, AIAA Paper 70-229, 1970.
[107] C.E. Peters, W.J. Phares, An approximate analysis of the shock structure in under-expanded plumes, Technical Report, Defense Documentation Center, 1976.
[108] M.D. Salas, The numerical calculation of inviscid plume flow fields, AIAA Paper 74 (523) (1974).
[109] Wen S. Young, Derivation of the free-jet Mach-disk location using the entropy-balance principle, Phys. Fluids 18 (11) (1975) 1421–1425.
[110] A. Alam, T. Setoguchi, Effect of inflow conditions on under-expanded supersonic jets, Int. J. Eng. Appl. Sci. 4 (1) (2012) 17–30.
[111] Er-yun Chen, Da-wei Ma, Gui-gao Le, Kai Wang, Gai-ping Zhao, Numerical simulation of highly underexpanded axisymmetric jet with Runge–Kutta discontinuous Galerkin finite element method, J. Hydrodyn. Ser. B 20 (5) (2008) 617–623.
[112] S.M. Dash, R.D. Thorpe, Shock-capturing model for one- and two-phase supersonic exhaust flow, AIAA J. 19 (7) (1981) 842–851.
[113] P. Dubs, M. Khalij, R. Benelmir, A. Tazibt, Study on the dynamical characteristics of a supersonic high pressure ratio underexpanded impinging ideal gas jet through numerical simulations, Mech. Res. Commun. 38 (3) (2011) 267–273.
[114] I.A. Graur, T.G. Elizarova, J.C. Lengrand, Numerical computation of shock wave configurations in underexpanded viscous jets, in: 22nd International Symposium on Shock Wave, 1999, pp. 1–25.
[115] T. Irie, T. Yasunobu, H. Kashimura, T. Setogushi, Characteristics of the Mach disk in the underexpanded jet in which the back pressure continuously changes with time, J. Therm. Sci. 12 (2) (2003) 132–137.
[116] G. Lehnasch, P. Bruel, A robust methodology for RANS simulations of highly underexpanded jets, Int. J. Numer. Methods Fluids 56 (12) (2008) 2179–2205.
[117] S. Matsuo, M. Tanaka, Y. Otobe, H. Kashimura, H.-D. Kim, T. Setoguchi, Effect of axisymmetric sonic nozzle geometry on characteristics of supersonic air jet,

Please cite this article as: E. Franquet, et al., Free underexpanded jets in a quiescent medium: A review, Progress in Aerospace Sciences (2015), http://dx.doi.org/10.1016/j.paerosci.2015.06.006

J. Therm. Sci. 13 (2) (2004) 121–126.
[118] S. Matsuo, Y. Otobe, M. Tanaka, H. Kashimura, T. Setoguchi, S. Yu, Effect of non-equilibrium condensation on axisymmetric under-expanded jet, Int. J. Turbo Jet Engines 21 (2004) 193–201.
[119] F. Nasuti, R. Niccoli, M. Onofri, A numerical methodology to predict exhaust plumes of propulsion nozzles, J. Fluids Eng., Trans. ASME 120 (3) (1998) 563–569.
[120] S.M. Prudhomme, H. Haj-Hariri, Investigation of supersonic underexpanded jets using adaptive unstructured finite elements, Finite Elem. Anal. Des. 17 (June (1)) (1994) 21–40.
[121] Alexey Velikorodny, Sergey Kudriakov, Numerical study of the near-field of highly underexpanded turbulent gas jets, Int. J. Hydrog. Energy 37 (22) (2012) 17390–17399.
[122] M.A. Woodmansee, V. Iyer, J.C. Dutton, R.P. Lucht, Nonintrusive pressure and temperature measurements in an underexpanded sonic jet flowfield, AIAA J. 42 (6) (2004) 1170–1180.
[123] N.I. Kislyakov, A.K. Rebrov, R.G. Sharafutdinov, Structure of high-pressure low-density jets beyond a supersonic nozzle, J. Appl. Mech. Tech. Phys. 16 (1975) 187–195.
[124] V.I. Nemchenko, N.I. Yushchenkova, Structure of low-density supersonic jet, J. Appl. Mech. Tech. Phys. 10 (6) (1969) 941–945.
[125] W. Davidor, S.S. Penner, Shock standoff distances and Mach-disk diameters in underexpanded sonic jets, AIAA J. 9 (8) (1971) 1651–1653.
[126] L. D'Attore, F. Harshbarger, Parameters affecting the normal shock location in underexpanded gas jets, AIAA J. 3 (3) (1965) 530.
[127] J.C. Lengrand, J. Allègre, M. Raffin, Experimental investigation of under expanded exhaust plumes, AIAA J. 14 (1976) 692–694.
[128] V.I. Nemchenko, Investigation of the closing shock in a supersonic submerged underexpanded gas jet, J. Eng. Phys. 20 (5) (1971) 648–654.
[129] B.A. Sodek, ATM optical contamination study, Technical Report, Research Laboratories Brown Engineering Company, 1968.
[130] Heuy-Dong Kim, Min-Sung Kang, Yumiko Otobe, Toshiaki Setoguchi, The effect of nonequilibrium condensation on hysteresis phenomenon of under-expanded jets, J. Mech. Sci. Technol. 23 (3) (2009) 856–867.
[131] E. Franquet, V. Perrier, S. Gibout, P. Bruel, Free underexpanded jets in a quiescent medium: a review, Technical Report, Univ. Pau & Pay Adour, 2015.
[132] K.J. Badcock, B.E. Richards, M.A. Woodgate, Elements of computational fluid dynamics on block structured grids using implicit solvers, Prog. Aerosp. Sci. 36 (5–6) (2000) 351–392.
[133] E.H. Andrews, A.R. Vick, C.B. Craidon, Theoretical boundaries and internal characteristics of exhaust plumes from three different supersonic nozzles, Technical Note D-2650, NASA, 1965.
[134] M. Belan, S. De Ponte, S. Massaglia, D. Tordella, Experiments and numerical simulations on the mid-term evolution of hypersonic jets, Astrophys. Space Sci. 293 (2004) 225–232.
[135] M. Belan, S. De Ponte, D. Tordella, Determination of density and concentration from fluorescent images of a gas flow, Exp. Fluids 45 (2008) 501–511.
[136] I.S. Belotserkovets, V.I. Timoshenko, Calculating the boundaries of a supersonic nonviscous jet entering a submerged space or a companion supersonic flow, J. Eng. Phys. 40 (2) (1981) 109–113.
[137] Frederick Boynton, Alex Thomson, Numerical computation of steady, supersonic, two-dimensional gas flow in natural coordinates, J. Comput. Phys. 3 (3) (1969) 379–398.
[138] T.T. Bui, CFD analysis of nozzle jet plume effects on sonic boom signature, TM 214650, NASA, 2009.
[139] V.G. Dulov, G.I. Smirnova, Calculation of the principal parameters of free supersonic jets of an ideal compressible fluid, J. Appl. Mech. Tech. Phys. 12 (3) (1971) 387–392.
[140] A.V. Ivanov, N.V. Stankus, S.F. Chekmarev, Hypersonic multicycle gas jet with a high degree of underexpansion at the nozzle exit, Fluid Dyn. 19 (6) (1984) 880–888.
[141] F.P. Boynton, Highly underexpanded jet structure: exact and approximate calculations, AIAA J. 5 (9) (1967) 1703–1704.
[142] J. Hartmann, F. Lazarus IV, The air-jet with a velocity exceeding that of sound, Philos. Mag. Ser. 7 31 (204) (1941) 35–50.
[143] K.A. Phalnikar, R. Kumar, F.S. Alvi, Experiments on free and impinging supersonic microjets, Exp. Fluids 44 (5) (2008) 819–830.
[144] V.M. Aniskin, A.A. Maslov, S.G. Mironov, Effect of nozzle size on supersonic microjet length, Tech. Phys. Lett. 37 (11) (2011) 1046–1048.
[145] Vladimir Aniskin, Sergey Mironov, Anatoliy Maslov, Investigation of the structure of supersonic nitrogen microjets, Microfluid. Nanofluid. 14 (3–4) (2013) 605–614.
[146] C.K.W. Tam, H.K. Tanna, Shock associated noise of supersonic jets from convergent–divergent nozzles, J. Sound Vib. 81 (3) (1982) 337–358.
[147] T.S. Cheng, K.S. Lee, Numerical simulations of underexpanded supersonic jet and free shear layer using WENO schemes, Int. J. Heat Fluid Flow 26 (5) (2005) 755–770.
[148] S.G. Chuech, M.-C. Lai, G.M. Faeth, Structure of turbulent sonic underexpanded free jets, AIAA J. 27 (5) (1989) 549–559.
[149] S.D. Scroggs, G.S. Settles, An experimental study of supersonic microjets, Exp. Fluids 21 (6) (1996) 401–409.
[150] K.B.M.Q. Zaman, Asymptotic spreading rate of initially compressible jets—experiment and analysis, Phys. Fluids 10 (10) (1998) 2652–2660.
[151] S. Clement, E. Rathakrishnan, Characteristics of sonic jets with tabs, Shock Waves 15 (3–4) (2006) 219–227.
[152] S.A. Novopashin, A.L. Perepelkin, Axial symmetry loss of a supersonic preturbulent jet, Phys. Lett. A 135 (1989) 290–293.
[153] P.O. Witze, A generalised theory for the turbulent mixing of axially symmetric compressible free jets, in: Fluids Mechanics of Mixing, 1973, pp. 63–77.
[154] P.O. Witze, Centerline velocity decay of compressible free jets, AIAA J. 12 (4) (1974) 417–418.
[155] J.W. Shirie, J.G. Seubold, Length of supersonic core in high-speed jets, AIAA J. 5 (11) (1967) 2062–2064.
[156] Tieh-Feng Hu, D.K. McLaughlin, Flow and acoustic properties of low Reynolds number underexpanded supersonic jets, J. Sound Vib. 141 (3) (1990) 485–505.
[157] S.A. Arnette, M. Samimy, G.S. Elliott, On streamwise vortices in high Reynolds number supersonic axisymmetric jets, Phys. Fluids A 5 (1) (1993) 187–202.
[158] E. Gutmark, K.C. Schadow, C.J. Bicker, Mode switching in supersonic circular jets, Phys. Fluids A: Fluid Dyn. 1 (5) (1989) 868–873.
[159] V.A. Kochnev, I.M. Naboko, Flat supersonic underexpanded jets using a laser schlieren method, J. Appl. Mech. Tech. Phys. 24 (1) (1983) 49–56.
[160] A. Krothapalli, P.J. Strykowski, C.J. King, Origin of streamwise vortices in supersonic jets, AIAA J. 36 (5) (1998) 869–872.
[161] V.Ya. Levchenko, V.M. Fomin, Aerogasdynamic investigations at the institute of theoretical and applied mechanics in the last decade, J. Appl. Mech. Tech. Phys. 38 (4) (1997) 535–565.
[162] V.A. Mal'tsev, S.A. Novopashin, A.L. Perepelkin, Effect of the plenum-chamber diameter on the turbulent characteristics of a supersonic jet, J. Appl. Mech. Tech. Phys. 40 (6) (1999) 1057–1060.
[163] O.A. Nerushev, S.A. Novopashin, A.L. Perepelkin, Transition to turbulence in supersonic jets of nitrogen and argon, Fluid Dyn. 33 (3) (1998) 459–462.
[164] J. Panda, Shock oscillation in underexpanded screeching jets, J. Fluid Mech. 363 (1) (1998) 173–198.
[165] V.N. Zaikovskii, S.P. Kiselev, V.P. Kiselev, Large-scale streamwise vortices in the supersonic part of a permeable nozzle, J. Appl. Mech. Tech. Phys. 46 (5) (2005) 670–676.
[166] V.I. Zapryagaev, A.V. Solotchin, Three-dimensional structure of flow in a supersonic underexpanded jet, J. Appl. Mech. Tech. Phys. 32 (1991) 503–507, http://dx.doi.org/10.1007/BF00851550.
[167] V.I. Zapryagaev, S.G. Mironov, A.V. Solotchin, Spectral composition of wave numbers of longitudinal vortices and characteristics of flow structure in a supersonic jet, J. Appl. Mech. Tech. Phys. 34 (5) (1993) 634–640.
[168] V.I. Zapryagaev, A.V. Solotchin, Development of streamwise vortices in the initial section of a supersonic non-isobaric jet in the presence of microroughness of the inner nozzle surface, Fluid Dyn. 32 (3) (1997) 465–469.
[169] V.I. Zapryagaev, A.V. Solotchin, An experimental investigation of the nozzle roughness effect on streamwise vortices in a supersonic jet, J. Appl. Mech. Tech. Phys. 38 (1) (1997) 78–86.
[170] V.I. Zapryagaev, A.V. Solotchin, N.P. Kiselev, Structure of a supersonic jet with varied geometry of the nozzle entrance, J. Appl. Mech. Tech. Phys. 43 (4) (2002) 538–543.
[171] V. Zapryagaev, V. Pickalov, N. Kiselev, A. Nepomnyashchiy, Combination interaction of Taylor–Goertler vortices in a curved shear layer of a supersonic jet, Theor. Comput. Fluid Dyn. 18 (2004) 301–308, http://dx.doi.org/10.1007/s00162-004-0141-5.
[172] V.I. Zapryagaev, N.P. Kiselev, A.A. Pavlov, Effect of streamline curvature on intensity of streamwise vortices in the mixing layer of supersonic jets, J. Appl. Mech. Tech. Phys. 45 (3) (2004) 335–343.
[173] V.I. Zapryagaev, A.P. Petrov, A.V. Solotchin, Investigation of nonuniformity of the velocity distribution in the shear layer of an underexpanded jet by electric discharge tracing of the flow, J. Appl. Mech. Tech. Phys. 45 (6) (2004) 822–827.
[174] V.I. Zapryagaev, A.V. Solotchin, Spectral characteristics of unstable flow in the mixing layer of supersonic underexpanded jet over its initial region, Thermophys. Aeromech. 16 (2) (2009) 209–218.
[175] S.M. Dash, R.G. Wilmoth, H.S. Pergament, An overlaid viscous/inviscid model for the prediction of near field jet entrainment, AIAA J. 17 (1979) 950–958.
[176] S.M. Dash, D.E. Wolf, Interactive phenomena in supersonic jet mixing problems. Part II: numerical studies, AIAA J. 22 (10) (1984) 1395–1404.
[177] L.L. Smarr, M.L. Norman, K.-H.A. Winkler, Shocks, interfaces, and patterns in supersonic jets, Physica D: Nonlinear Phenom. 12 (1–3) (1984) 83–106.
[178] N.M. Terekhova, Effect of flow nonparallelism on instability of the Taylor–Görtler waves in supersonic axisymmetric jets, J. Appl. Mech. Tech. Phys. 41 (4) (2000) 604–611.
[179] N.M. Terekhova, Nonlinear group interactions of the Taylor–Görtler disturbances in supersonic axisymmetric jets, J. Appl. Mech. Tech. Phys. 45 (5) (2004) 647–655.
[180] N.A. Zheltukhin, N.M. Terekhova, Disturbances of high modes in a supersonic jet, J. Appl. Mech. Tech. Phys. 31 (2) (1990) 232–239.
[181] N.A. Zheltukhin, N.M. Terekhova, Taylor–Görtler instability in a supersonic jet, J. Appl. Mech. Tech. Phys. 34 (5) (1993) 640–647.
[182] H. Oertel Sen, F. Seiler, J. Srulijes, New explanation of noise production by supersonic jets with gas dredging, in: Andreas Dillmann, Gerd Heller, Michael Klaas, Hans-Peter Kreplin, Wolfgang Nitsche, Wolfgang Schröder (Eds.), New Results in Numerical and Experimental Fluid Mechanics VII, Notes on Numerical Fluid Mechanics and Multidisciplinary Design, vol. 112, Springer, Berlin, Heidelberg, 2010, pp. 389–397.
[183] H. Oertel Sen, F. Seiler, J. Srulijes, Vortex induced Mach waves in supersonic jets, in: Konstantinos Kontis (Ed.), 28th International Symposium on Shock Waves, Springer, Berlin, Heidelberg, 2012, pp. 657–663.
[184] J. Panda, R.G. Seasholtz, Measurement of shock structure and shock-vortex interaction in underexpanded jets using Rayleigh scattering, Phys. Fluids 11 (12) (1999) 3761–3777.
[185] H. Oertel Sen, F. Seiler, J. Srulijes, Visualization of Mach waves produced by a supersonic jet and theoretical explanations, J. Vis. 16 (4) (2013) 303–312.
[186] C.J. Moore, The role of shear-layer instability waves in jet exhaust noise, J. Fluid Mech. 80 (321–367) (1977) 4.
[187] H.K. Tanna, W.H. Brown, C.K.W. Tam, Shock associated noise of inverted-profile coannular jets, part I: experiments, J. Sound Vib. 98 (1) (1985) 95–113.
[188] C.K.W. Tam, H.K. Tanna, Shock associated noise of inverted-profile coannular jets, part II: condition for minimum noise, J. Sound Vib. 98 (1) (1985) 115–125.
[189] C.K.W. Tam, H.K. Tanna, Shock associated noise of inverted-profile coannular jets, part III: shock structure and noise characteristics, J. Sound Vib. 98 (1) (1985) 127–145.
[190] C.K.W. Tam, Supersonic jet noise, Annu. Rev. Fluid Mech. 27 (1) (1995) 17–43.
[191] N.E. Afonina, S.A. Vasil'evskii, V.G. Gromov, A.F. Kolesnikov, I.S. Pershin, V. I. Sakharov, M.I. Yakushin, Flow and heat transfer in underexpanded air jets issuing from the sonic nozzle of a plasma generator, Fluid Dyn. 37 (5) (2002) 803–814.
[192] I.D. Boyd, P.F. Penko, D.L. Meissner, K.J. Dewitt, Experimental and numerical investigations of low-density nozzle and plume flows of nitrogen, AIAA J. 30 (10)

Please cite this article as: E. Franquet, et al., Free underexpanded jets in a quiescent medium: A review, Progress in Aerospace Sciences (2015), http://dx.doi.org/10.1016/j.paerosci.2015.06.006

(1992) 2453–2461.
[193] C.B. Devaud, J.B. Kelman, J.B. Moss, C.D. Stewart, Stability of underexpanded supersonic jet flames burning H_2-CO mixtures, Shock Waves 12 (2002) 241–249.
[194] J. Dubois, M. Amielh, F. Anselmet, O. Gentilhomme, Investigation of axisymmetric underexpanded air and helium jets by background oriented schlieren, J. Vis. 12 (2009) 192.
[195] R.E. Foglesong, S.M. Green, R.P. Lucht, J.C. Dutton, Dual-pump coherent anti-stokes Raman scattering for simultaneous pressure/temperature measurement, AIAA J. 36 (2) (1998) 234–240.
[196] A.N. Gordeev, A.F. Kolesnikov, V.I. Sakharov, Flow and heat transfer in underexpanded nonequilibrium jets of an induction plasmatron, Fluid Dyn. 46 (4) (2011) 623–633.
[197] Kenneth Harstad, Josette Bellan, Global analysis and parametric dependencies for potential unintended hydrogen-fuel releases, Combust. Flame 144 (1–2) (2006) 89–102.
[198] V.A. Ivanov, G.A. Luk'yanov, I.V. Shatalov, Effect of rarefaction and the temperature factor on the structure and parameters of supersonic underexpanded jets of a monatomic gas, J. Appl. Mech. Tech. Phys. 28 (1987) 859–863.
[199] N.I. Kislyakov, A.K. Rebrov, R.G. Sharafutdinov, Diffusion processes in the mixing zone of a supersonic jet of low density, J. Appl. Mech. Tech. Phys. 14 (1) (1973) 99–104.
[200] K. Kurita, T. Okai, K. Ueno, N. Kawada, M. Kato, Velocity and temperature distributions in an underexpanded supersonic jet by using a laser induced fluorescence, Anal. Sci. 7 (1991) 1459–1462.
[201] L.I. Kuznetsov, A.K. Rebrov, V.N. Yarygin, High-temperature jets of low-density argon beyond a sonic nozzle, J. Appl. Mech. Tech. Phys. 16 (1975) 378–382.
[202] P. Lovaraju, E. Rathakrishnan, Effect of cross-wire location on the mixing of underexpanded sonic jets, J. Aerosp. Eng. 20 (3) (2007) 179–185.
[203] P.V. Marrone, Temperature and density measurements in free jet and shock waves, Phys. Fluids 10 (1967) 521–538.
[204] B. Maté, G. Tejeda, S. Montero, Raman spectroscopy of supersonic jets of CO_2: density, condensation, and translational, rotational, and vibrational temperatures, J. Chem. Phys. 108 (7) (1998) 2676–2685.
[205] B. Maté, I.A. Graur, T. Elizarova, I. Chirokov, G. Tejeda, J.M. Fernández, S. Montero, Experimental and numerical investigation of an axisymmetric supersonic jet, J. Fluid Mech. 426 (2001) 177–197.
[206] V.V. Volchkov, A.V. Ivanov, N.I. Kislyakov, A.K. Rebrov, V.A. Sukhnev, R.G. Sharafutdinov, Low-density jets beyond a sonic nozzle at large pressure drops, Zh. Prikl. Mekh. Tekhn. 2 (64–73) (1973).
[207] K.B. Yüceil, M.V. Ötügen, Scaling parameters for underexpanded supersonic jets, Phys. Fluids 14 (12) (2002) 4206–4215.
[208] V.N. Gusev, T.V. Klimova, V.V. Ryabov, Similarity of flows in strongly underexpanded jets of viscous gas, Izvetiya Akad. Nauk SSSR, Mekh. Zhidkosti i Gaza 6 (117–125) (1977).
[209] A.N. Kraiko, On the free unsteady expansion of an ideal gas, Fluid Dyn. 28 (4) (1993) 553–559.
[210] P.L. Owen, C.K. Thornhill, The flow in an axially-symmetric supersonic jet from a nearly sonic orifice into a vacuum, Technical Report, British Aeronautical Research Council, 1952.
[211] V.V. Riabov, Aerodynamic applications of underexpanded hypersonic viscous jets, J. Aircr. 32 (3) (1995) 471–479.
[212] I. Al-Qadi, J.N. Scott, Simulations of unsteady behavior in under-expanded supersonic rectangular jets, AIAA Paper, 2001, p. 2119.
[213] P.S. Cumber, M. Fairweather, S.A.E.G. Falle, J.R. Giddings, Predictions of impacting sonic and supersonic jets, J. Fluids Eng. 119 (1997) 83–89.
[214] S.M. Dash, B.E. Pearce, H.S. Pergament, E.S. Fishburne, Prediction of rocket plume flow fields for infrared signature studies, J. Spacecr. Rockets 17 (1960) 190–199.
[215] S.M. Dash, D.E. Wolf, J.M. Seiner, Analysis of turbulent underexpanded jets, part I: parabolized Navier–Stokes model, SCIPVIS, AIAA J. 23 (1985) 505–514.
[216] M. Fairweather, K.R. Ranson, Prediction of underexpanded jets using compressibility-corrected, two-equation turbulence models, Prog. Comput. Fluid Dyn. 6 (1–3) (2006) 122–128.
[217] Andrew T. Hsu, Meng-Sing Liou, A computational analysis of under-expanded jets in the hypersonic regime, J. Propuls. Power 7 (2) (1991) 297–299.
[218] S.A. Isaev, Yu.M. Lipnitskii, P.A. Baranov, A.V. Panasenko, A.E. Usachov, Simulation of a turbulent supersonic underexpanded jet flowing into a submerged space with the help of a shear stress transfer model, J. Eng. Phys. Thermophys. 85 (2012) 1357–1371.
[219] M.L. Norman, L. Smarr, K.-H.A. Winkler, M.D. Smith, Structure and dynamic of supersonic jets, Astron. Astrophys. 113 (1982) 285–302.
[220] W.L. Oberkampf, M. Talpallikar, Analysis of a high-velocity oxygen-fuel (HVOF) thermal spray torch part 1: numerical formulation, J. Therm. Spray Technol. 5 (1) (1996) 53–61.
[221] W.L. Oberkampf, M. Talpallikar, Analysis of a high-velocity oxygen-fuel (HVOF) thermal spray torch part 2: computational results, J. Therm. Spray Technol. 5 (1) (1996) 62–68.
[222] A. Palacio, M.R. Malin, N. Proumen, L. Sanchez, Numerical computations of steady transonic and supersonic flow fields, Int. J. Heat Mass Transf. 33 (6) (1990) 1193–1204.
[223] E. Venkatapathy, W.J. Feiereisen, 3-D plume flow computations with an upwind solver, AIAA Paper 88 (3158) (1988).
[224] A.D. Birch, D.R. Brown, M.G. Dodson, F. Swaffield, The structure and concentration decay of high pressure jets of natural gas, Combust. Sci. Technol. 36 (5) (1984) 249–261.
[225] A.D. Birch, D.J. Hughes, F. Swaffield, Velocity decay of high pressure jets, Combust. Sci. Technol. 52 (1987) 161–171.
[226] J. Chaineaux, G. Mavrothalassitis, J. Pineau, Modelization and validation of the discharge in air of a vessel pressurized by flammable gas, Prog. Astronaut. Aeronaut. 134 (1991) 104–137.
[227] J.P. Gore, G.M. Faeth, Structure and radiation properties of large-scale natural gas/air diffusion flames, Fire Mater. 10 (1986) 161–169.
[228] Philip G. Hill, Patric Ouellette, Transient turbulent gaseous fuel jets for diesel engines, J. Fluids Eng. 121 (1) (1999) 93–101.
[229] G.T. Kalghatgi, Blow-out stability of gaseous jet diffusion flames. Part I: in still air, Combust. Sci. Technol. 26 (5–6) (1981) 233–239.
[230] E. Papanikolaou, D. Baraldi, M. Kuznetsov, A. Venetsanos, Evaluation of notional nozzle approaches for CFD simulations of free-shear under-expanded hydrogen jets, Int. J. Hydrog. Energy 37 (23) (2012) 18563–18574.
[231] E. Ruffin, Y. Mouilleau, J. Chaineaux, Large scale characterization of the concentration field of supercritical jets of hydrogen and methane, J. Loss Prev. Process Ind. 9 (4) (1996) 279–284.
[232] P.D. Sunavala, C. Hulse, M.W. Thring, Mixing and combustion in free and enclosed turbulent jet diffusion flames, Combust. Flame 1 (2) (1957) 179–193.
[233] J.D. Cole, Note on the axisymmetric sonic jet, SIAM J. Appl. Math. 43 (4) (1983) 944–948.
[234] William Houf, Robert Schefer, Predicting radiative heat fluxes and flammability envelopes from unintended releases of hydrogen, Int. J. Hydrog. Energy 32 (1) (2007) 136–151.
[235] W.G. Houf, G.H. Evans, R.W. Schefer, Analysis of jet flames and unignited jets from unintended releases of hydrogen, Int. J. Hydrog. Energy 34 (14) (2009) 5961–5969.
[236] Renato Benintendi, Turbulent jet modelling for hazardous area classification, J. Loss Prev. Process Ind. 23 (3) (2010) 373–378.
[237] J.-B. Saffers, V.V. Molkov, Towards hydrogen safety engineering for reacting and non-reacting hydrogen releases, J. Loss Prev. Process Ind. 26 (2) (2013) 344–350.
[238] Ivar Øyvind Sand, Karl Sjøen, Jan Roar Bakke, Modelling of release of gas from high pressure pipelines, Int. J. Numer. Methods Fluids 23 (9) (1996) 953–983.
[239] R.W. Schefer, W.G. Houf, T.C. Williams, B. Bourne, J. Colton, Characterization of high-pressure, underexpanded hydrogen-jet flames, Int. J. Hydrog. Energy 32 (12) (2007) 2081–2093.
[240] D.M. Webber, M.J. Ivings, R.C. Santon, Ventilation theory and dispersion modelling applied to hazardous area classification, J. Loss Prev. Process Ind. 24 (5) (2011) 612–621.
[241] W.S. Winters, G.H. Evans, Final report for the ASC gas–powder two-phase flow modeling project, Technical Report, Sandia National Laboratories Report No. SAND2006-7579, 2007.
[242] D. Baraldi, E. Papanikolaou, M. Heitsch, P. Moretto, R.S. Cant, D. Roekaerts, S. Dorofeev, A. Koutchourko, P. Middha, A.V. Tchouvelev, S. Ledin, J. Wen, A. Venetsanos, V. Molkov, Gap analysis of CFD modelling of accidental hydrogen release and gap analysis of CFD modelling of accidental hydrogen release and combustion, Technical Report, European Commission, Joint Research Centre, Institute of Energy, 2010.
[243] William H. Calhoon Jr, Computational assessment of afterburning cessation mechanisms in fuel rich rocket exhaust plume, J. Propuls. Power 17 (1) (2001) 111–119.
[244] P. Middha, O.R. Hansen, I.E. Storvik, Validation of CFD-model for hydrogen dispersion, J. Loss Prev. Process Ind. 22 (6) (2009) 1034–1038.
[245] P. Ouellette, P.G. Hill, Turbulent transient gas injections, J. Fluids Eng. 122 (4) (2000) 743–752.
[246] A. Rusin, K. Stolecka, Modelling the effects of failure of pipelines transporting hydrogen, Chem. Process Eng. 32 (2) (2011) 117–134.
[247] A. Veser, M. Kuznetsov, G. Fast, A. Friedrich, N. Kotchourko, G. Stern, M. Schwall, W. Breitung, The structure and flame propagation regimes in turbulent hydrogen jets, Int. J. Hydrog. Energy 36 (3) (2011) 2351–2359.
[248] J. Xiao, J.R. Travis, W. Breitung, Hydrogen release from a high pressure gaseous hydrogen reservoir in case of a small leak, Int. J. Hydrog. Energy 36 (3) (2011) 2545–2554.
[249] Jinyang Zheng, Haiyan Bie, Ping Xu, Pengfei Liu, Yongzhi Zhao, Honggang Chen, Xianxin Liu, Lei Zhao, Numerical simulation of high-pressure hydrogen jet flames during bonfire test, Int. J. Hydrog. Energy 37 (1) (2012) 783–790.
[250] M.W. Thring, M.P. Newby, Combustion length of enclosed turbulent jet flames, in: Fourth Symposium (International) on Combustion, vol. 4(1), 1953, pp. 789–796.
[251] V. Molkov, Hydrogen safety engineering: the state-of-the-art and future progress, in: Ali Sayigh (Ed.), Compr. Renew. Energy, vol. 4, Elsevier, Oxford, 2012, pp. 77–109.
[252] G. Kleinstein, Mixing in turbulent axially symmetric free jets, J. Spacecr. Rockets 1 (1964) 403–408.
[253] W.R. Warren, An Analytical and Experimental Study of Compressible Free Jets, Report N. 381, University of Princeton, 1957.
[254] C.J. Chen, W. Rodi, Vertical Turbulent Buoyant Jets—A Review of Experimental Data, Pergamon Press, 1980.
[255] M.P. Davis, A.C.H. Mace, N.C. Markatos, On numerical modelling of embedded subsonic flow, Int. J. Numer. Methods Fluids 6 (3) (1986) 103–112.
[256] B. Emami, M. Bussmann, H.N. Tran, A mean flow field solution to a moderately under/over-expanded turbulent supersonic jet, Comptes Rendus Mécanique 337 (4) (2009) 185–191.
[257] P.O. Jarvinen, J.S. Draper, Underexpanded gas-particle jets, AIAA J. 5 (4) (1967) 824–825.
[258] Hylton R. Murphy, David R. Miller, Effects of nozzle geometry on kinetics in free-jet expansions, J. Phys. Chem. 88 (20) (1984) 4474–4478.
[259] A.D. Rychkov, Flow of a mixture of gas and solid particles in supersonic underexpanded jets, Fluid Dyn. 9 (1974) 224–227.
[260] J.A. Schetz, F.S. Billig, Penetration of gaseous jets injected into a supersonic stream, J. Spacecr. 3 (11) (1966).
[261] Sheldon Weinbaum, Richard W. Garvine, On the two-dimensional viscous counterpart of the one-dimensional sonic throat, J. Fluid Mech. 39 (01) (1969) 57–85.
[262] R. Ishii, Y. Umeda, M. Yuhi, Numerical analysis of gas-particle two-phase flows, J. Fluid Mech. 203 (1989) 475–515.
[263] Kaveh Mohamed, Marius Paraschivoiu, Real gas simulation of hydrogen release from a high-pressure chamber, Int. J. Hydrog. Energy 30 (8) (2005) 903–912.
[264] V.I. Pogorelov, G.B. Shcherbanina, Discharge of a supersonic jet from a nozzle with an inclined rim, Fluid Dyn. 12 (4) (1977) 572–576.
[265] R. Sinha, V. Zakhay, J. Erdos, Flowfield analysis of plumes of two dimensional underexpanded jets by a time dependent method, AIAA J. 9 (1971) 2363–2370.
[266] V.N. Vetlutsky, V.L. Ganimedov, M.I. Muchnaya, Influence of the opening angle of a conical supersonic nozzle on the structure of initial interval of non-isobaric jet, Thermophys. Aeromech. 15 (2) (2008) 197–203.

Please cite this article as: E. Franquet, et al., Free underexpanded jets in a quiescent medium: A review, Progress in Aerospace Sciences (2015), http://dx.doi.org/10.1016/j.paerosci.2015.06.006

[267] Y. Bartosiewicz, Zine Aidoun, P. Desevaux, Yves Mercadier, Numerical and experimental investigations on supersonic ejectors, Int. J. Heat Fluid Flow 26 (1) (2005) 56–70.
[268] P.S. Cumber, M. Fairweather, S.A.E.G. Falle, J.R. Giddings, Predictions of the structure of turbulent, moderately underexpanded jets, J. Fluids Eng. 116 (4) (1994) 707–713.
[269] S. Dembele, J. Zhang, J.X. Wen, Exploratory study of under-expanded sonic hydrogen jets and jet flames, in: Proceedings of the 5th International Seminar on Fire and Explosion Hazards, 2007.
[270] D.A. Dickmann, F.K. Lu, Jet in supersonic crossflow on a flat plate, in: 25th AIAA Aerodynamic Measurement Technology and Ground Testing Conference, vol. 2, 2006, pp. 981–992.
[271] Sujith Sukumaran, Song-Charng Kong, Numerical study on mixture formation characteristics in a direct-injection hydrogen engine, Int. J. Hydrog. Energy 35 (15) (2010) 7991–8007.
[272] V.N. Vetlutsky, V.L. Ganimedov, M.I. Muchnaya, Flow in a viscous jet escaping through a supersonic nozzle into a semi-infinite ambient space, J. Appl. Mech. Tech. Phys. 50 (6) (2009) 918–926.
[273] E. Yamada, S. Watanabe, A.K. Hayashi, N. Tsuboi, Numerical analysis on auto-ignition of a high pressure hydrogen jet spouting from a tube, Proc. Combust. Inst. 32 (2) (2009) 2363–2369.
[274] M.V. Bragin, V.V. Molkov, Physics of spontaneous ignition of high-pressure hydrogen release and transition to jet fire, Int. J. Hydrog. Energy 36 (3) (2011) 2589–2596 (The Third Annual International Conference on Hydrogen Safety).
[275] G. Lacaze, B. Cuenot, T. Poinsot, M. Oschwald, Large eddy simulation of laser ignition and compressible reacting flow in a rocket-like configuration, Combust. Flame 156 (6) (2009) 1166–1180.
[276] D.A. Lyubimov, Development and applications of the efficient hydrid RANS/ILES approach for the calculation of complex turbulent jets, High Temp. 46 (2) (2008) 243–253.
[277] D. Munday, E. Gutmark, J. Liu, K. Kailasanath, Flow structure and acoustic of supersonic jets from conical convergent–divergent nozzles, Phys. Fluids 23 (11) (2011) 116102.
[278] J.X. Wen, B.P. Xu, V.H.Y. Tam, Numerical study on spontaneous ignition of pressurized hydrogen release through a length of tube, Combust. Flame 156 (11) (2009) 2173–2189.
[279] J.A. Boles, J.R. Edwards, R.A. Bauerle, Large-Eddy/Reynolds-averaged Navier–Stokes simulations of sonic injection into mach 2 crossflow, AIAA J. 48 (7) (2010) 1444–1456.
[280] D. Cecere, A. Ingenito, E. Giacomazzi, L. Romagnosi, C. Bruno, Hydrogen/air supersonic combustion for future hypersonic vehicles, Int. J. Hydrog. Energy 36 (18) (2011) 11969–11984.
[281] A. Dauptain, E. Gutmark, J. Liu, K. Kailasanath, Large-Eddy simulation of a stable supersonic jet impinging on flat plate, AIAA J. 48 (10) (2010) 2325–2337.
[282] S. Kawai, S.K. Lele, Large-Eddy simulation of jet mixing in supersonic crossflows, AIAA J. 48 (2010) 2063–2083.
[283] T. Nakano, M.D. Mahbubul Alam, S. Matsuo, M. Tanaka, T. Setoguchi, Effect of heterogeneous condensation on axisymmetric supersonic free jets, in: Proceedings of the International Conference on Mechanical Engineering, 2005.
[284] K.D. Kihm, T.K. Kim, S.Y. Son, Visualization of high-speed gas jets and their airblast sprays of cross-injected liquid, Exp. Fluids 27 (1) (1999) 102–106.
[285] Seung-Cheol Baek, Soon-Bum Kwon, Heuy-Dong Kim, Toshiaki Setoguchi, Shigeru Matsuo, Study of moderately underexpanded supersonic moist air jets, AIAA J. 44 (7) (2006) 1624–1627.
[286] P.S. Cumber, Predicting outflow from high pressure vessels, Process Saf. Environ. Protect. 79 (1) (2001) 13–22.
[287] M. Epstein, H.K. Fauske, Total flammable mass and volume within a vapor cloud produced by a continuous fuel-gas or volatile liquid-fuel release, J. Hazard. Mater. 147 (3) (2007) 1037–1050.
[288] M.S. Ivanov, D. Vandromme, V.M. Fomin, A.N. Kudryavtsev, A. Hadjadj, D.V. Khotyanovsky, Transition between regular and Mach reflection of shock waves: new numerical and experimental results, Shock Waves 11 (3) (2001) 199–207.
[289] P.V. Marrone, Rotational temperature and density measurements in underexpanded jets and shock waves using an electron beam probe, Technical Report, Institute for Aerospace Studies, 1966.
[290] M. Kuznetsov, Hydrogen distribution tests in free turbulent jet. Technical Report, FZK, SBEP V4, 2006.
[291] K. Okabayashi, T. Nonaka, N. Sakata, K. Takeno, H. Hirashima, K. Chitose, Characteristics of dispersion for leakage of high-pressurized hydrogen gas, Jpn. Soc. Saf. Eng. 44 (2005) 391–397.
[292] L.C. Shirvill, P. Roberts, C.J. Butler, T.A. Roberts, M. Royle, Characterisation of the hazards from jet releases of hydrogen, in: First International Conference on Hydrogen Safety, 2005.

Please cite this article as: E. Franquet, et al., Free underexpanded jets in a quiescent medium: A review, Progress in Aerospace Sciences (2015), http://dx.doi.org/10.1016/j.paerosci.2015.06.006